Manuscript

Click here to download Manuscript
Revised_PONE_D_161370_Dubois.docx

Microevolution of Bank Voles (*Myodes glareolus*) at Neutral and Immune-Related Genes During Multiannual Dynamic Cycles: Consequences for Puumala hantavirus Epidemiology

Adelaïde Dubois[1,2*], Maxime Galan[1], Jean-François Cosson[1,3], Bertrand Gauffre[4], Heikki Henttonen[5], Jukka Niemimaa[5], Maria Razzauti[1], Liina Voutilainen[5,6], Renaud Vitalis[1], Emmanuel Guivier[7], Nathalie Charbonnel[1]

[1] INRA, UMR CBGP, F-34988 Montferrier-sur-Lez, France

[2] Anses, Unité de Virologie, 31 avenue Tony Garnier, 69364 Lyon, France

[3] INRA-ANSES-ENVA, UMR 0956 BIPAR, Maisons-Alfort, France.

[4] INRA, USC1339 (CEBC-CNRS), Villiers en Bois F-79360, France

[5] Natural Resources Institute Finland, FI-013012 Vantaa, Finland

[6] Department of Virology, University of Helsinki, FI-00014 University of Helsinki, Finland

[7] Biogeosciences, CNRS UMR 6282, Université de Bourgogne, Franche-Comté, 21000 Dijon, France

* Email: adelaide.dubois@supagro.inra.fr

Short title: Microevolution of Bank Vole Metapopulation

Keywords: population genetics; immune-related gene; host pathogen interaction; microevolution; dynamic fluctuations; Puumala virus; rodent; *Myodes glareolus*; bank vole; epidemiology; adaptation; selection

Abstract

Understanding how host dynamics, including spatiotemporal variations of population size and dispersal, may affect the epidemiology of infectious diseases is an active research area. Population dynamics drive neutral and adaptive micro-evolutionary processes that in turn, influence pathogens persistence, their distribution and evolution. This study focuses on a bank vole (*Myodes glareolus*) metapopulation surveyed in Finland between 2005 and 2009. Bank vole is the reservoir of Puumala hantavirus (PUUV), the agent of nephropathia epidemica (NE, a mild form of hemorrhagic fever with renal symptom) in humans. *M glareolus* populations experience multiannual density fluctuations that influence the level of genetic diversity maintained in bank voles, variations in PUUV prevalence and NE occurrence in humans. Here, we examine bank vole metapopulation genetics at presumably neutral markers and immune-related genes (*Tnf*-promoter, *Mhc-Drb, Tlr4*, *Tlr7* and *Mx2* gene). We discuss its potential consequences on PUUV epidemiology. Using microsatellites, we show that genetic drift slightly and transiently affects neutral and adaptive genetic variability within the metapopulation. Gene flow seems to counterbalance its effects during the multiannual density fluctuations. The low abundance phase may therefore be too short to impact genetic variation in the host, and consequently viral genetic diversity. Environmental heterogeneity does not seem to affect vole gene flow, which might explain the absence of spatial structure previously detected in PUUV in this area. We find evidence for the role of vole dispersal on PUUV circulation through sex-specific and density-dependent movements. We also analyze how density cycles affect selection acting on immune-related genes involved in susceptibility to PUUV. We detect associations between *Mhc-Drb* haplotypes and PUUV serology, and between Mx2 genotype and PUUV genogroups. We also find footprint of positive selection at *Tlr-4* gene in 2008 only. These results emphasize the potential interactions between bank vole immunogenetics and PUUV microevolution.

Introduction

Molecular epidemiology has largely focused on the parasite side, contributing to a better understanding of transmission patterns and factors influencing disease spread. From the host side, population genetics can also be of great importance to analyze pathogen persistence, spread and evolution, although it has been overlooked (1). Indirect approaches based on host population genetics can highlight local variations in genetic diversity that are due to demographic fluctuations of effective population size, a central parameter in epidemiology. Besides, many parasites lack free-living stages or have limited dispersal capacities and are therefore highly dependent of their hosts to disperse (2). When disease transmission is specifically associated with a given host species, host population genetics can reveal environmental heterogeneity that may affect the spread of diseases by reducing both movements of infected hosts and contacts between infected and non-infected ones (3). Studies on landscape genetics in the host could therefore help predicting this spread of diseases and developing proactive disease management. The analysis of adaptive genetic variation, especially that linked to host–pathogen interactions, should also improve our knowledge of disease epidemiology (see for a review (4). For example, immune-related gene polymorphism may be affected by genetic drift (e.g (5–7), but several studies have revealed that balancing selection, in addition to migration, could rapidly buffer the loss of adaptive diversity (e.g. *Mhc* heterozygosity) in bottlenecked populations (8,9).

The development of host population genetics in epidemiological contexts might be highly relevant when populations exhibit multiannual density cycles. Such dynamics can lead to variations of effective population size (10) that may significantly affect genetic diversity and population genetic structure. Drastic reductions in population size can cause a rapid decrease of allelic richness and a gradual erosion of heterozygosity, with negative consequences on adaptive potential (11–13). However a high level of genetic diversity may sometimes persist in these populations, both at neutral and immune-related genes (9,14–18). Density cycles can also impact dispersal rates, and consequently the distribution of genetic variability within and among populations. Several studies showed that cyclic populations of the fossorial water vole were weakly differentiated during the increasing phase of abundance, suggesting high migration rate among

demes, but highly differentiated during the low phase of abundance, as a result of local genetic drift and low dispersal rates (15,19). Such cyclic dynamics could therefore have severe consequences on disease epidemiology, both ecologically and evolutionarily. Up to now, most of the studies dedicated to the genetics of these cyclic populations have been done in the context of agricultural damages. The links with epidemiological risks still remain to be explored.

In this study, we examined this tripartite relationship between host density cycles, population genetics and epidemiology of a viral infection in the bank vole (*Myodes glareolus*) and Puumala hantavirus (PUUV, family of *Bunyaviridae*) as model species. In boreal Fennoscandia, bank vole populations undergo three to five year density cycles with high amplitude (20,21). The bank vole is the reservoir of PUUV, the etiologic agent of nephropathia epidemica (NE) (22). Among voles, the virus is transmitted horizontally through direct contacts between individuals (*i.e*. bites) or indirectly via infectious aerosolized urine and feces (23,24). The spread of PUUV is therefore closely linked to its host dispersal. PUUV infection in bank voles is chronic and mainly asymptomatic (25–27) as maturation, winter survival and female breeding of infected individuals may be affected (28–30). The epidemiology of PUUV in rodent populations has been well documented (31). Only two studies have yet examined the connection between bank vole population and genetic microevolution of PUUV. Guivier et al. (32) developed a landscape genetics approach in temperate zone to analyze the influence of bank vole population dynamics on PUUV spatial distribution in contrasted landscape structures. They considered genetic diversity as a proxy for estimating vole population size, isolation and migration, and found that it was highly positively correlated with PUUV prevalence and with the abundance of forest habitats at a local scale. This suggested that the persistence of PUUV was enhanced in lowly fragmented forests, where vole metapopulations are highly connected and experience low extinction rates. This result was congruent with previous correlations found between human PUUV incidence and coverage of beech tree forests (33). Besides, Weber de Melo et al. (34) made a comparative analysis of the spatiotemporal population genetic structure of bank voles and PUUV at a smaller spatial scale. They aimed at testing the influence of vole neutral microevolutionary processes on PUUV

phylodynamics. They found incongruent patterns between host and PUUV population genetic structure that were likely to arise due to the high evolutionary rate of this virus.

What is still missing to better understand the links between PUUV epidemiology and bank vole metapopulation dynamics is the characterization of the microevolutionary processes at play in the genes known to influence rodent susceptibility to hantaviruses (review in (35). To bridge this gap, we analyzed the genetics of bank voles at presumably neutral and immune-related genes in a metapopulation monitored during a whole demographic cycle in an highly endemic NE area of Finland. We first examined the consequences of drastic density variations on the dynamics of neutral and adaptive genetic diversity in *M. glareolus* populations, both at the metapopulation scale and at a finer scale. Second, we performed population genetics analyses to look for spatial barriers, like lake or rivers, that could affect gene flow within the bank vole metapopulation and therefore the circulation of PUUV. We also tested whether PUUV transmission was likely to result from vole dispersal or contacts between relatives (36). Third, we sought to disentangle the effects of drift, migration and selection acting on vole immune-related genes. To this aim, we compared the genetic structure observed at these genes to that measured at presumably neutral microsatellite markers, assuming that differences between the two could be the consequence of selection. We also looked for associations between immune-related gene polymorphism, susceptibility to PUUV and PUUV genetic variants. These latter analyses enabled to investigate the possibility that selective forces may shape bank vole / PUUV interactions despite the pronounced multiannual density cycles.

Materials and Methods

Ethic statement

All handling procedures of wild live bank voles followed the Finnish Act on the Use of Animals for Experimental Purposes (62/2006) and took place with permission from the Finnish Animal Experiment Board (license numbers HY 45-02, HY 122-03, and HY 54-05). All efforts were made to minimize animal suffering. The species captured for this study, *Myodes glareolus*, neither is

protected nor included in the Red List of Finnish Species. The animal trapping took place with permission from the landowners.

Rodent sampling and PUUV detection

Rodents were trapped within an area of about 25 km² of typical spruce-dominated taiga forest at Konnevesi, Central Finland (62° 34’ N, 26° 24’ E), where PUUV is highly endemic (28,31,37–39). Trappings for bank vole genetic materials were carried out between 2005 and 2009 to include a whole density cycle (peak year 2005, decline 2006, increase 2007, peak 2008, decline 2009, see (17,25,39), Fig. 1). Too few individuals could be sampled in crash year 2006 so that individuals sampled in 2006 were not included in the study. Trapping sessions were conducted in the beginning and middle period of the breeding season (May, July in 2005, 2008, 2009) or in October (2007, 2009) to gather enough individuals when abundance levels were low. Nine sites situated at least 750m apart from each other within 25 km^2 were sampled (Fig. 1). Briefly, a grid of 3 x 3 Ugglan Special live traps (Grahnab AB, Sweden) with 15 m intervals and baited with oat seeds and potato was set in each site. Traps were checked once a day during three days, and captured bank voles were brought into the laboratory, bled through retro-orbital sinus, sacrificed, weighed, measured and sexed (for details, see Voutilainen et al. (31). Tissue samples (toe or tip of the tail) were collected and stored in 95% ethanol for further genetic analyses. The heart of each animal was collected, diluted into 200 µL phosphate-buffered saline and frozen for latter PUUV antibody analysis. Detection of PUUV was done as described in Kallio-Kokko et al. (40). Serological and virological data have previously been described in Voutilainen et al. (25,31) and Razzauti et al. (39,38). Because PUUV infection in bank voles is chronic, the presence of PUUV antibodies was taken as an indicator of infection (27), except for juvenile voles trapped in July because of the possible presence of maternal antibodies (41). In this case, seropositive bank voles with low body mass (<17.5g, see Voutilainen et al. (31) were considered juveniles carrying maternal antibodies but not PUUV infected (21 bank voles were concerned and were not considered in the analyses including seroprevalence). Sampling size and seroprevalence levels are described in details in Table S1.

Fig 1. Map of the study area and long-term fluctuations of bank voles in Konnevesi. A) The nine trapping sites included in this study are indicated by a red square. These sites were situated at least 750 m apart. The location of Konnevesi within Finland is shown on the right box. B) Total bank vole abundance and number of infected voles trapped per 100 trap nights in the nine Konnevesi sites considered in this study between 2005 and 2009 (from (31). White circles represent sampling dates. This figure contains data from the National Land Survey of Finland Topographic Database 06/2013 (left panel) and Esri, HERE, and DeLorme (right panel).

DNA extraction and loci amplification

Microsatellite analyses – We analyzed 402 bank voles. Genomic DNA was extracted using the DNeasy 96 Tissue kit (Qiagen) according to manufacturer's recommendations. A final elution was done in 400µl of AE buffer (Qiagen). Samples were first genotyped at 19 unliked microsatellites loci previously published by Rikalainen et al. (42) using primers and cycling conditions described in Guivier et al. (32). Genotyping was carried out using an ABI3130 automated DNA sequencer (Applied Biosystems). Alleles were scored using GENEMAPPER software (Applied Biosystems). Two loci were excluded from the genetic analyses: Cg6G11 because of the poor quality profiles obtained and Cg5F11 because it was duplicated in these populations.

Candidate gene analyses - The polymorphism of candidate genes that are relevant with regard to PUUV infections was further analyzed. These candidate genes, namely *Mhc-Drb, Tlr4* and *Tlr7, Tnf-α* promoter and *Mx2* were selected based on the literature of rodent or human/hantavirus interactions (35,43). The second exon of the *Mhc-Drb* class II is a highly polymorphic gene of the major histocompatibility complex. It encodes for proteins responsible for pathogen recognition (44). *Tlr4* and *Tlr7* genes encode for Toll-like receptors which play an important role in activating the innate immune system (45). TLR4 is a universal receptor able to detect different ligands as LPS of Gram-negative bacteria and also some viral proteins (46) including hantaviral proteins (47). TLR7 is a receptor to virus, which is probably involved in the detection of ssRNA viruses like hantaviruses (48). As both *Mhc* and *Tlr* genes encode for receptors, their polymorphism is likely to

be linked to the efficiency of antigen recognition. *Tnf* (Tumour Necrosis Factor alpha) gene encodes for a cytokine involved in the pro-inflammatory response (49). Polymorphism within the *Tnf* promoter seems to be, at least partly, implicated in the regulation of *Tnf* transcription and consequently in the magnitude of the secretory response of this cytokine (50,51). Mx proteins are interferon-induced members of the superfamily of large GTPases. They mediate innate, antiviral resistance in rodents, as well as in other vertebrates and humans (52,53). Most Mx GTPases inhibit a wide range of RNA viruses, including members of the *Bunyaviridae* at an early stage in their life cycle. Thus, the efficiency of antiviral resistance seems to be mediated by *Mx* genes polymorphism.

The second exon of the *Mhc-Drb* class II was genotyped using a 454 Genome Sequencer FLX (Roche) with the procedure detailed in Galan et al. (54). The locus was amplified using a modified version of the primers JS1 (5'- GCCTCCCTCGCGCCATCAG -3') and JS2 (5'- GCCTTGCCAGCCCGCTCAG -3') initially designed for a lemur (55). Individual-specific MIDs (Multiplex Identifiers) and 454 adaptors required for the emPCR and the 454 GS-FLX sequencing were also added (for more details concerning laboratory procedures, see (54,56). The SESAME barcode software (SEquence Sorter & AMplicon Explorer (57) was used to sort sequences, identify and discard artefactual variants, and generate the allele sequences and individual genotypes. The *Drb*-exon2 sequences were aligned in the BioEdit sequence alignment editor (58) using CLUSTAL X Multiple Alignment v7.0.9.0 (59). Nomenclature of the bank vole sequences follows Klein et al. (60). The sequences are available in GenBank under accession numbers HM347503–HM347507 and HM107849–HM107870. Human *Homo sapiens* (GenBank accession numbers 91M17236 and AM109973), sheep *Ovis aries* (M33304, AY230000) and pig *Sus scrofa* (M29938, NM_001113695) sequences were used as outgroups in phylogenetic analyses. MEGA4 software (61) was employed to construct a phylogenetic tree of the *Drb*-exon2 gene using the neighbor-joining algorithm and Kimura two-parameter distance model. A bootstrap analysis (1000 replicates) was performed to determine the reliability of the branching. As previously described in Axtner & Sommer (62) and observed in Guivier et al. (63) and Rohfritsch et al. (43), one to six different haplotypes could be observed for a single bank vole, indicating the presence of duplications in the *Mhc-Drb*-exon2

gene, the number of which varies between individuals. The phylogenetic reconstructions did not enable us to assign all haplotypes to a particular copy of the *Mhc-Drb* gene (Supplementary Material Fig. S2). However, we confirmed that cluster I, first described by Axtner & Sommer (62), is highly supported (see also (64,65). We could therefore identify unambiguously the different haplotypes belonging to this monophyletic cluster. We also verified that each bank vole carried two haplotypes from cluster I at most, what highly corroborated the fact that it corresponds to a single *Mhc-Drb* gene copy. As it was not possible to delineate any other cluster, the remaining haplotypes were not considered in further population genetics analyses.

Polymorphisms of *Tnf* gene promoter (63), *Tlr4* and *Tlr7* gene, and *Mx2* exons 13 and 14, were previously investigated by the sequencing of bank voles sample from several European countries. Protocol S1 and Table S2 provide details on the list of primers and PCR conditions used to amplify the gene products. At the European scale, we identified ten single nucleotide polymorphisms (SNPs) in *Tlr4* exon 3, one SNP in *Tlr7* exon 3 and four SNPs in *Mx2* exons 13 and 14 (Table S2, (35,43). Based on this previous pilot study, we selected the eight polymorphic SNPs that were not singletons (haplotype frequencies higher than 5%, (66,67). Two of them were non-synonymous. The software PolyPhen (http://genetics.bwh.harvard.edu/ pph; (68) was used to predict the functional impact of these non-synonymous SNPs on the translated protein, based on biochemical and physical characteristics of the amino acid replacements. The 402 individuals from Konnevesi were genotyped at these SNPs using the KASPar allelic-specific fluorescent genotyping system provided by KBiosciences (Hoddesdon, UK).

Statistical analyses

Within site and within metapopulation genetic diversity – As the number of voles trapped per site could be low, we pooled samples from May and July for each site. Moreover, because 2009 was a low-density year, we pooled all samples from all sites between May and October for this year. Further analyses were realized at two different spatial scales for each year: for each site and over the whole metapopulation. Considering microsatellites, we tested the conformity to Hardy-Weinberg equilibrium (HWE) for each locus and we analyzed linkage disequilibrium (LD) for each

pair of loci using GENEPOP v4.2 (69). Corrections for multiple tests were performed using the false discovery rate (FDR) approach as described in Benjamini & Hochberg (70). For all microsatellites and for each immune gene (*Mhc-Drb, Tnf, Mx2*, *Tlr4* and *Tlr7*), we estimated $N_{a,}$ the estimate of allelic richness corrected for minimum sample size (8 in our case) (71,72), the observed (H_o) and Nei's unbiased expected (H_e) heterozygosities (73) and Weir & Cockerham's inbreeding coefficient F_{IS} (74). Significance of F_{IS} (excess or deficit in heterozygotes) was assessed using 1000 permutations of alleles within each site. Similar estimates were obtained over the whole metapopulation. Calculations and tests were realized using GENETIX v4.05.2 (75), using FDR corrections. For these analyses, the sites x years combinations with less than eight individuals were not considered in order to avoid statistical biases.

To test whether these indices of within site and metapopulation genetic diversity varied throughout the vole dynamic cycles, we focused on N_a and H_e and we defined two linear mixed models, using the lme function implemented in the nlme package for R 3.1.0 (76). Model validations were realized *a posteriori* by checking plots of the residuals. The first model included independently these indices of diversity estimated for the sites sampled in 2005, 2007 and 2008 (2009 was not included as sample sizes per site were too low). Fixed effects included the variables *year*, *site*, *type of loci* (microsatellites, SNPs, *Mhc-Drb*). We also included the pairwise interactions *year*type of loci* and *year*site*. When the pairwise interactions were non-significant, they were removed from the model. The variable *loci* was included as a random effect to reflect the fact that there were initial differences in diversity between loci. The second model included the indices of diversity calculated over the whole metapopulation for each year between 2005 and 2009 as response variables. The fixed effects *year*, *type of loci,* their pairwise interaction *year*type of loci* and the random effect *loci* were also added. For both models, significance of the fixed effects was assessed with analysis-of-deviance tables (function ANOVA). Chi-square tests with Bonferroni correction were then applied to analyze the effect of significant variables using the package phia for R.

Test for selective neutrality at microsatellite loci – We used the software package FDIST2 (77) to test for homogeneity in differentiation level across the final set of microsatellite loci (15 markers,

see the Results section). This method is based on the principle that genetic differentiation among populations (as measured by F_{ST}) is expected to be higher for loci under divergent selection, and lower for loci under balancing selection, as compared to the rest of the genome. The rationale of FDIST2 is to compute F_{ST} and the overall heterozygosity at each marker (computed as the average pairwise difference between all possible pairs of genes between each sample), and then to compare these values to a null distribution, generated by means of neutral coalescent simulations in a symmetrical island model at migration-drift equilibrium. Since the method was applied on microsatellite data, we used a stepwise mutation model, as implemented in FDIST2. One million simulations were performed for each analysis, assuming a 25-demes island model (and the same number of sampled demes as in the original dataset). Simulations were performed for each year independently. As in Ségurel et al. (78), we used the averaged shifted histogram (ASH) algorithm (79) to characterize the probability distribution, to provide a "high probability region" that contains 90%, 95%, or 99% of the total probability distribution, and to derive an empirical *p*-value for the joint (F_{ST}, H_e) estimates at the candidate genes.

Spatial genetic structure - We first evaluated the level of genetic isolation of each site relatively to the others using microsatellite markers. Population-specific F_{ST} values and their 95% confidence interval were estimated using the software GESTE (80). We then investigated the relationships between bank vole population dynamics and bank vole PUUV epidemiology using a logistic regression performed with the glm function implemented in R. PUUV seroprevalence was the response variable. We defined the explanatory variables as the two first principal components of a principal component analysis (PCA) of the genetic parameters (H_e, H_o, F_{ST}, F_{IS}, N_a) estimated for each site and each year.

Spatial genetic structure was described using genetic differentiation between each pair of sites estimated from microsatellite data and Weir & Cockerham's pairwise F_{ST} estimates (74). Temporal differentiation was evaluated by estimating F_{ST} values between sampling dates. We used exact tests implemented in GENEPOP v4.2 (69) to test for differentiation. FDR corrections were applied as described above. We next used analyses of molecular variance (AMOVA) implemented

in ARLEQUIN v3.5.1.2 (81) to quantity the proportions of genetic variation due to differences between years and between sites, using two hierarchical models (see Table 1 for details).

Spatial genetic clustering was performed using microsatellites markers in a single analysis including all years and sites to detect potential environmental factors affecting gene flow. We used the Bayesian clustering method implemented in STRUCTURE (82), using the admixture model with correlated allele frequencies. We performed 20 independent runs, varying the number of clusters from $K = 2$ to $K = 8$, using a Markov chain Monte Carlo (MCMC) made of 10^6 iterations following a burn-in of 500,000 iterations. To determine the number of clusters (K) best fitting our multilocus genetic data set, we used the method described in Evanno et al. (83). We next used the FullSearch algorithm implemented in CLUMPP v1.1 (84) to assign individuals to clusters. Then, summary bar plots were built using DISTRUCT v1.1 (85).

We finally examined the fine-scale spatial pattern of microsatellite genetic variation using inter-individual relatedness. We estimated the *Li* coefficient (86) implemented in SPAGEDI v1.4.c (87) for each year, considering each site separately. This estimator shows a high accuracy (low bias) combined with a high precision (low variance) compared to others (88). We performed spatial autocorrelation analyses to examine how genetic similarity between pairs of individuals changed with geographical distance. This approach was applied independently for each year, and separately for males and females to emphasize potential differences in the dispersal behavior with cycle phases (17,18). We next tested whether relatedness differed among seropositive and among seronegative bank voles, by permuting individuals between these two classes. The 15 seropositive juveniles carrying maternal antibodies were removed from this analysis. Because pairwise data are non-independent, we could not directly compare relatedness estimates between these classes of individuals using standard statistical tests (89). We thus applied the procedure of Coulon et al. (90) that consists in generating 1,000 random resampling sets without replacement, such that each individual occurs only once in a given resampled set. The difference of mean relatedness D_i between the two categories tested is then calculated for each resampling set. Under the null hypothesis, D_i should follow a normal distribution centered on 0; under the alternative hypothesis, D_i should be significantly different from 0. We made no *a priori* assumption on the sign of the

difference and thus computed two-sided tests. Indeed, on one hand, PUUV seropositive bank voles could be less related than seronegative ones if PUUV transmission mainly occurs during dispersal. On the other hand, the opposite pattern is expected if PUUV transmission occurs during winter family clustering, but up to now, this pattern has only been observed in temperate zones (see (91).

F_{ST} outlier test to detect signatures of selection in candidate genes – We evaluated whether the genetic differentiation at immune-related genes (*Mhc-Drb* and SNPs) departed from the null distribution expected at neutrality. The rationale was to compute F_{ST} and the overall heterozygosity at each immune-related gene, and then to compare these values to a null distribution, obtained by means of neutral coalescent simulations in a symmetrical island model at migration-drift equilibrium. These simulations generated conditionally on the overall F_{ST} estimate calculated from the microsatellite markers (F_{ST} = 0.0209 in 2005; F_{ST} = 0.0182 in 2007 and F_{ST} = 0.0252 in 2008). Therefore, the null distribution is independent from the level of differentiation observed at the candidate genes. For the analysis of the *Mhc-Drb* data, we considered each haplotype as an allele, and we used FDIST2 (which is specifically designed for the analysis of multiallelic data) to test for departure from the neutral distribution. For the analysis of the SNP data, we used a version of the software package DFDIST, which we modified to generate bi-allelic co-dominant data (78). An infinite allele model of mutation was considered, with $\theta = 2nN\mu = 0.1$ (where $n = 25$ is the number of demes of size N, and μ is the mutation rate). Only the simulations resulting in bi-allelic data were retained. One million simulations were performed for each analysis, assuming a 25-demes island model (and the same number of sampled demes as in the original dataset). For all simulations, the maximum frequency of the most common allele allowed was set to 0.99. These analyses were realized for each year independently. We characterized the “high probability regions” (based on the the level of differentiation at neutral markers) and the empirical *p*-values at the candidate genes using the averaged shifted histogram (ASH) algorithm (79), as in Ségurel et al. (78). Because the true demographic history of *M. glareolus* populations is likely to depart from the underlying assumptions of FDIST2 and the modified DFDIST, especially with respect to the hypothesis of stable

population size, we investigated to what extent the approach to detect signatures of selection was robust to temporal variations in population size (see Supplementary Appendix S1).

Association between genotypes at immune-related genes and PUUV serology - Because candidate gene polymorphism was expected to be related to bank vole susceptibility to PUUV, we searched for associations between immune variations and PUUV serology which was used as a proxy of PUUV infection status (63). This analysis was realized on the whole dataset, from which we excluded the 14 seropositive juveniles carrying maternal antibodies. First, we performed a correspondence analysis (CoA) on the genetic matrix of candidate gene polymorphism (*Mhc-Drb*: haplotypes; other candidate genes: SNPs, coded as presence/absence), using the software ADE-4 (92). Then, we realized a discriminant function analysis (DA) using PUUV serology as a discriminant factor. The significance of the analysis was estimated by using 10,000 permutation tests. The relative risk (RR) associated with each allele of interest, as detected with DA, was estimated following (93). The significance of the association between these alleles and vole serological status were analyzed using Fisher exact tests and Bonferroni sequential corrections. Similar analyses were performed for seropositive bank voles (N = 46) to look for potential associations between PUUV diversity (PUUV genogroups, see Razzauti et al. (39,38) and bank vole immune-related gene polymorphism.

Results

Validation of loci

Two microsatellite loci, Cg2F2 and Cg13F9, showed important deviations to HWE suggesting the presence of null alleles. They were removed from the analyses. Thus, our final dataset included 402 bank vole genotypes at 15 microsatellites loci. The analyses performed using FDIST2 revealed that none of these microsatellites departed from neutral expectation (Supplementary Material Fig. S1).

The 454 sequencing of *Mhc-Drb* exon 2 revealed 17 haplotypes belonging to the monophyletic allele cluster I (62), Supplementary Material Fig. S2). We did not observe more than

two haplotypes from this cluster per individual, what corroborates the fact that these genotypes corresponded to a unique *Mhc-Drb* gene copy. Eighteen variable sites were detected among the 171 bp sequences, out of which eight corresponded to non-synonymous sites.

Eight SNPs were genotyped over all other candidate genes: Four SNPs appeared to be monomorphic over the five SNPs analyzed within *Tlr4* and were excluded from the data. No polymorphism was found within *Tlr7.* Finally, polymorphism of a single SNP was analyzed for each of the following immune-related genes: *Mx2*, *Tnf* promoter and *Tlr4*. This apparently low number of polymorphic SNPs is not due to insufficient genotyping quality, the KASPar allele-specific fluorescent genotyping system provided by Kbiosciences being robust. In fact, it is likely to result from the very small spatial scale of our study (25 km2 within a single forest), as observed for field voles in Kielder Forest for example (94).

Within site and within metapopulation genetic diversity

A total of 43 pairs of microsatellites exhibited significant LD over the 684 tested (6%) after FDR correction. The loci involved were not consistent among years and sites. Two out of 60 tests for deviation from HWE were significant, and both concerned the locus Cg16H5.

Table S1 gives the range of diversity estimates, across years and sites, and at the whole metapopulation scale, for microsatellites markers and immune-related genes. Detailed results of the statistical models performed on diversity indices are presented in Table S4. Briefly, H_e and N_a estimates were always higher at microsatellite loci than at immune-related genes (Within site - H_e: $X^2_2 = 45.69$, $p < 10^{-4}$; N_a: $X^2_2 = 25.72$, $p < 10^{-4}$; Within metapopulation - H_e: $X^2_2 = 169.20$, $p < 10^{-4}$; N_a: $X^2_2 = 19.48$, $p = 10^{-4}$, see Fig. 2). At the local scale (within site), H_e estimates also varied among years ($X^2_2 = 8.47$, $p = 0.015$), with lower estimates observed in 2008 than in 2007, and they marginally varied among sites ($X^2_4 = 9.575$, $p = 0.048$). Other factors than *type of loci* explained variation in N_a estimates at the metapopulation scale only. Hence N_a estimates within metapopulation varied among years ($X^2_3 = 8.985$, $p = 0.029$), with lower estimates observed in 2009 compared to 2005. We noted that the loss of alleles was of similar amplitude at microsatellites and *Mhc-Drb* (about two alleles lost over 12 between 2005 and 2009, Table 1).

Interestingly, one *Mhc-Drb* variant was lost during the crash between 2005 and 2007, and was not recovered at the metapopulation scale the years after. Contrastingly, new *Mhc-Drb* haplotypes were detected in particular sites of the metapopulation in 2008 (e.g. Mygl-DRB*15 in site M and Mygl-DRB*08 in site F). Immune SNPs exhibited strong temporal changes compared to other loci (interaction *year* * *type of loci:* X^2_6 = 41.67, $p < 10^{-4}$), in particular for *Mx2*_162 and *Tlr4*_1662, where higher H_e levels were explained by the increased frequency of the less common variant (from 0.25 to 0.35 and 0.21 to 0.34 respectively).

Fig 2. Temporal variations of H_e *and* N_a estimates (mean ± SD) for the whole metapopulation, by type of locus.

Microsatellite loci are represented as triangles, *Mhc-Drb* as circle and SNPs as square. A linear mixed model was performed with the four diversity indices estimated over the whole metapopulation sampled in 2005, 2007, 2008 and 2009. Significant differences between years are indicated by asterisks (* $p < 0.05$; *** $p < 0.001$).

Spatial genetic structure

Site-specific F_{ST} estimates at microsatellite markers (computed using the GESTE software) ranged between 0.009 and 0.063, showing various levels of genetic isolation of sites within the bank vole metapopulation (Table S1). The first axis of the PCA based on microsatellite genetic parameters (PC1) explained 57.4% of the variability and revealed a strong opposition between these local F_{ST} estimates and the other genetic features describing genetic diversity, especially H_e and N_a (Fig 3A). This axis therefore illustrated the opposing impacts of genetic drift and migration on local genetic diversity. The second axis of the PCA (PC2) accounted for 36.5% of the total variability, and opposed microsatellite genetic parameters reflecting the deviation from Hardy-Weinberg equilibrium within site (H_o and F_{is}). The third PCA axis (PC3) explained 5.1% of the variability and contrasted the diversity indices N_a and H_e (Fig 3B). The projection of the variable *year* on this axis revealed that PC3 discriminated the increase phase 2007 after the decline in 2006 and peak years (2005, 2008). The best and the most parsimonious model explaining PUUV prevalence using site

coordinates on these three axes included PC3 only (*z*-value = 2.119, *p* = 0.034). PUUV prevalence therefore seemed mostly related to local changes in microsatellite allelic richness associated with the population cycle, PUUV seroprevalence reaching higher levels during the increase year (2007).

Fig 3. Principal component analysis based on local genetic parameters estimated using microsatellites.

Correlation circles of the five genetic variables using A) PC1 and PC2, and B) PC1 and PC3. Puumala seroprevalence was included as a supplementary variable.

Spatial pairwise F_{ST} estimates ranged between 0.003 and 0.056 for microsatellites, -0.077 and 0.270 for SNPs and -0.067 and 0.109 for *Mhc-Drb*. While most of these estimates were not significant after FDR correction for microsatellites (84.5%), a few remained significant when considering respectively SNPs and *Mhc-Drb* (Table S5). At the scale of the metapopulation, temporal pairwise F_{ST} ranged between 0.003 and 0.017 at microsatellites, with high estimates corresponding to pairs of sampling date including the crash year 2009. None of these estimates were significant when considering immune-related genes (Table S6).

AMOVA analyses revealed an absence of temporal genetic differentiation over the whole metapopulation whatever the loci considered, but significant variation among years within sites, with higher percentage of variation detected at *Mhc-Drb* than at microsatellites. No temporal genetic changes were detected at immune-related SNPs (Table 1A, B). Over the whole survey, AMOVA revealed a weak spatial genetic structure detected using microsatellites only, and significant variation among sites within years for all loci, with higher percentage of variation detected at *Mhc-Drb* than at microsatellites or immune-related SNPs (Table 1A, B).

Table 1. Analysis of molecular variance (AMOVA).

AMOVA were performed considering the five sites B, C, F, G, O sampled in 2005, 2007 and 2008 (sample size larger than 8 individuals) and the three types of loci, *i.e.* microsatellites, immune

SNPs and *Mhc-Drb*. Two hierarchies were examined: A) years as groups and sites as subdivisions within years; B) sites as groups and years as subdivisions within sites.

A)

	Microsatellites				SNPs				*Mhc-Drb*			
Source of variation	*DF*	Variance components	Percentage of variation	*p*	*DF*	Variance components	Percentage of variation	*p*	*DF*	Variance components	Percentage of variation	*p*
Among years	2	-0.003	-0.04	0.731	2	-0.004	-0.743	0.865	2	-0.002	-0.394	0.761
Among sites within years	12	0.166	2.570	**$<10^{-5}$**	12	0.009	1.966	**0.036**	12	0.019	4.516	**$<10^{-5}$**
Among individuals within sites	449	6.292	97.47	**$<10^{-5}$**	443	0.482	98.78	0.064	399	0.412	95.88	**$<10^{-5}$**

B)

	Microsatellites				SNPs				*Mhc-Drb*			
Source of variation	DF	Variance components	Percentage of variation	p	DF	Variance components	Percentage of variation	p	DF	Variance components	Percentage of variation	p
Among sites	4	0.042	0.65	**0.0006**	4	-0.003	-0.553	0.677	4	0.002	0.378	0.424
Among years within sites	10	0.128	1.98	**$<10^{-5}$**	10	0.009	1.914	0.064	10	0.017	3.908	**0.001**
Among individuals within year	449	6.292	97.37	**$<10^{-5}$**	443	0.482	98.64	0.066	399	0.412	95.88	**$<10^{-5}$**

Clustering analyses based on microsatellites performed over the whole dataset revealed three clusters that did not discriminate either years or sites. All voles were assigned to these three genotypic groups (Fig 4A, B). It is therefore likely that a complete absence of spatiotemporal structure (K = 1) is the best hypothesis to explain this result.

Fig 4. STRUCTURE plots of the bank vole metapopulation over the whole survey

The figure presents A) the bar plots resulting from the clustering analysis based on microsatellites and performed for K = 3 on bank voles sampled over the whole survey. Within bar plots, each individual is represented by a single vertical line broken into K colored segments, which lengths are proportional to the individual membership coefficients, in each inferred cluster. Each color represents a different genotypic group. B) The rate of change in the log probability of the data

between successive *K* values (Δ(*K*) *i.e.* L''(*K*) divided by the standard deviation of L(*K*)) is shown for *K* = 2 to *K* = 9.

Spatial autocorrelograms revealed a strong decrease of relatedness between individuals with geographic distance, whatever the sex and year considered (Fig 5). Nevertheless, mean relatedness of females was slightly higher at very small spatial scale (within sampling site or in the first surrounding sites distant from less than 1 km) during peak years (respectively 0.04 and 0.05 in 2005 and 2008) than during the increase phase (0.03 in 2007). Contrastingly, relatedness between males was higher within sites during the increase phase (0.03) than during peak years (respectively 0.01 and 0.02 in 2005 and 2008). For each year, the estimates of mean relatedness among seropositive and seronegative voles in the metapopulation showed very low and similar values, respectively r = -0.006 and $r = 6.10^{-4}$ in 2005 (p = 0.344), r = -0.014 and r = -0.006 in 2007 (p = 0.857), r = -0.009 and r = 0.005 in 2008 (p = 0.333) and r = -0.050 and r = 0.030 in 2009 (p = 0.399).

Fig 5. Spatial autocorrelation analyses based on Li's relatedness coefficient.
Correlograms are presented independently for males and females and for each year of sampling between 2005 and 2008. Geographic distances classes are indicated in km. The mean and standard error of Li's relatedness coefficient (86) are indicated for each class.

Detection of signatures of selection

The patterns of differentiation conditional on heterozygosity differed between genes and years. Departures from neutral expectation were observed in 2007 and 2008, at immune-related SNPs only: we found some locus-specific F_{ST} estimates lying outside the 95% or the 90% confidence region of the null distribution (Fig 6). In 2007, the *Tnf*-296 SNP was more differentiated (F_{ST} = 0.122) than expected under neutrality (Fig. 6B), showing a marginally significant footprint of positive selection (p = 0.090). In 2008, the *Tlr4*-1662 SNP was more differentiated (F_{ST} = 0.076) than expected under neutrality (Fig. 6C), showing a significant signature of positive selection (p =

0.037). *Mx2*-162 SNP exhibited low F_{ST} estimates (F_{ST} = -0.030 in 2007; F_{ST} = -0.013 in 2008), showing a marginally significant footprint of balancing selection in 2008 (p = 0.090). No significant departure from neutral expectations was found for *Mhc-Drb*, whatever the year considered (Figs. 6D-F). Investigating to what extent the approach to detect signatures of selection was robust to temporal variations in population size, we found virtually no difference between the distributions of F_{ST} conditional on heterozygosity across different scenarios of population size changes (see Supplementary Material Fig. S3), which justifies *a posteriori* the use of our approach to detect signatures of selection on cyclic populations.

Fig 6. Distribution of F_{ST} conditional on the overall heterozygosity (H_e) at immune-related genes, for the whole metapopulation dataset in 2005, 2007 and 2008. Black dots represent the observed, locus-specific, estimates of differentiation and heterozygosity for SNPs in candidate genes (A-C) and for *Mhc-Drb* (D-F). The 90%, 95% and 99% confidence regions of the null distribution (obtained by means of stochastic simulations in a neutral model) are shown in dark grey, medium grey and light grey, respectively. The density was obtained using the average shifted histogram (ASH) algorithm (79) with smoothing parameter m = 2.

Associations between immune-related genotypes and PUUV

Immune gene polymorphism marginally discriminated PUUV seropositive and seronegative voles (p = 0.077). Five alleles of the *Mhc-Drb* gene tended to be associated with PUUV serological status. The RR values of Mygl-DRB*106, Mygl-DRB*08 and Mygl-DRB*94 reached respectively 1.724, 1.717 and 1.464, indicating that individuals carrying this allele were almost twice more likely to be PUUV seropositive than others (Fig 7). On the contrary, with a respective RR value of 0.263 and 0.339, bank voles carrying Mygl-DRB*105 and Mygl-DRB*15 were more than twice less likely to be PUUV seropositive than others (Fig 7). However, after Bonferroni sequential corrections, these RR values were not significant. Note that similar results were observed when considering only over-wintered bank voles that had a long time of potential exposure to PUUV (results not shown).

We also found a marginally significant association between bank vole polymorphism at *Mx2*-162 SNP (presence/absence of G) and PUUV genogroup. Individuals carrying the G nucleotide at *Mx2*-162 SNP were at higher risk of being infected with PUUV reassortants (S segment, genogroup A & M segment genogroup B or S segment, genogroup B & M segment genogroup A ; RR = 7.500, p = 0.052) than those carrying the C base only. The within/between analysis confirmed the importance of this *Mx2*-162 SNP on PUUV polymorphism (Fig. 7C).

Fig 7. Discriminant analysis performed on immune-related polymorphism of PUUV adult bank voles over the whole metapopulation.

A) PUUV seropositive adult bank voles, represented by black dot, are marginally different from PUUV-seronegative ones, represented by white dot. B) Alleles indicated in bold (Mygl-DRB*106, Mygl-DRB*08, Mygl-DRB*94, Mygl-DRB*15 and Mygl-DRB*105) are associated with PUUV serological status. C) Representation of the two first axes of the within/between analysis performed on seropositive adult bank voles only, with A, B, R corresponding to the PUUV genogroups defined by Razzauti et al. (39,38) and immune-related gene polymorphisms indicated by blue dots.

Discussion

In this study, we analysed the genetic variation of a bank vole metapopulation, experiencing three-year population density cycles, at microsatellite loci and immune-related genes to examine the potential impact of microevolutionary processes on PUUV epidemiology. Overall, we showed that neutral and adaptive genetic variability was maintained through years despite repeated demographic bottlenecks. Rapid increase in vole density and high gene flow seemed to counterbalance the effects of genetic drift, which may explain the absence of founder effects observed in PUUV populations throughout vole population cycles. Despite this strong influence of demographic processes, selection also participated in driving immune-related gene polymorphism. Complex patterns were observed according to the immune-related genes and cycle phases considered. More specifically, we found that *Mhc-Drb* alleles tend to be associated with PUUV

serology. Furthermore, we characterized some departures from neutral expectations, and associations between PUUV genetic variants and bank vole alleles at immune-related genes (*Tnf*, *Tlr4* and *Mx2*), which could reflect signatures of positive and/or balancing selection. The latter patterns differed between years corresponding to different phases of the density cycles.

Genetic drift, bank vole dispersal and PUUV epidemiology

In boreal Fennoscandia, bank vole populations experience strong multiannual fluctuations in abundance, with peaks occurring every three to five years and abundance varying by a factor 500 between low and peak phases (95). Such regular and severe declines in population size are expected to affect neutral genetic variation through genetic drift. However, several studies have shown that cyclic rodent populations maintained high levels of genetic diversity, at least at a metapopulation scale (9,16,18,19,96,97). Marginal and temporal decreases in allelic richness were previously observed by Rikalainen et al. (17), who studied Finnish bank vole populations at a larger scale (100 km^2) around Konnevesi. Our results provided similar patterns, with high levels of heterozygosity and allelic richness being observed whatever the cycle phase considered. We detected a decrease in allelic richness in the crash phase of 2009 at the scale of the metapopulation. This loss of diversity might be only transient as no decrease could be observed after the 2006 crash year. Therefore, fluctuations in population size did not lead to strong signature of bottleneck in the genetic data, whatever the spatial scale considered. Similarly, Razzauti et al. (39) did not find any evidence of founder effects affecting PUUV diversity in the area including this vole metapopulation. Significant loss of PUUV variants were detected in 2009 only, with the complete absence of variants from one of the two PUUV genogroups otherwise detected since 2005. These patterns could be explained by the low sampling size in 2009. But it is likely that the low phase is usually too short to impact host genetic diversity, and/or that strong bank vole gene flow might compensate for genetic drift (16). Genetic patterns of temporal and spatial differentiation supported the hypothesis that dispersal among sites may rapidly counterbalance the potential loss of genetic diversity experienced by vole and PUUV populations. Although significant temporal genetic differentiation was locally detected between years, low estimates of temporal genetic

differentiation were detected at the scale of the metapopulation. These estimates were slightly higher when comparing pairs of sampling dates before and after decline (especially in 2009). This result corroborated the transient impact of genetic drift on the distribution of genetic variability, and the importance of gene flow occurring after population crash, once vole population size increased again. The relative temporal genetic stability of this metapopulation was also supported by the clustering analysis performed over the whole survey, as it did not reveal any spatial consistent structuring. Altogether, these results emphasized the absence of environmental heterogeneity within the studied area, a typical boreal forest, that could disrupt bank vole gene flow and in turn, PUUV dispersal among sites. The possibility for voles to move all around this area provides an explanation for the absence of spatial structure detected in PUUV population across this area (39).

Spatial autocorrelation analyses highlighted changes in the bank vole spatial genetic structure from year to year, that probably resulted from density fluctuations favouring dispersal and population turnover (e.g. (16,17). This raised the question of density-dependent dispersal, that is, whether dispersal rate increased during low phase or with increasing population size (see Pilot et al. (98) for references and predictions). As evidenced by Rikalainen et al. (17) and Gauffre et al. (18), our study provided arguments in favour of sex-specific and density-dependence dispersal. Negative density dependent migration of females could underlie the local changes in relatedness observed between low density and peak years. The slightly lower relatedness observed during the increase phase could hence be explained by the colonisation of new empty sites by females. The high levels of relatedness observed during 2005 and 2008 could reflect female phylopatry and low migration (see Le Galliard et al. (99) once population size has reached high abundance. On the other hand, the lower levels of relatedness observed in peak years compared to the increase phase when focusing on males could result from their high dispersal rate and high gene flow once density reached high levels. The social behavior in *M. glareolus* is likely to underlie these variations of dispersal through time. Dispersal is strongly connected with maturation, which is season and density-dependent. Maturation phases and connected dispersal of young maturing voles are shorter in the peak than in the increase summer, as they only concern the first litter produced in spring. This sex-biased density dependent migration could be of main importance in shaping

PUUV epidemiology. Indeed, a male bias in PUUV infection was detected in Konnevesi in overwintered, breeding bank voles, whereas a female bias was seen in summer-born breeding animals probably as a result of more frequent contact with old (infected) males or aggressive encounters with other breeding females during the territory establishment (31). In addition, PUUV seropositive voles were found to be more abundant during the high-density years of the dynamic cycle (increase and peak autumn - winters), as confirmed by the strong correlation observed in this study between PUUV seroprevalence and two indices of genetic diversity differentiating peak *versus* low-density years. We could therefore suggest that during low-density phase, female voles could play a role in the colonization of empty sites and consequently in the transmission of PUUV. During peak years, males would be responsible for repeated dispersal events and gene flow, therefore contributing to PUUV transmission.

Impact of metapopulation dynamics on immune-related gene polymorphism

Whether migration and natural selection can counterbalance the effect of drift on immune gene polymorphism in populations experiencing drastic fluctuations remains an open research topic, as empirical data have revealed contrasted patterns. From an eco-evolutionary perspective, this question is of uttermost importance as a loss of genetic variation could result in dampened adaptive capability, which is especially problematic when faced with rapidly evolving pathogens. A recent meta-analysis showed that a greater loss of genetic diversity was generally seen at *Mhc* genes rather than at neutral loci, potentially because of the uneven distribution of haplotypes before the bottleneck (6). Here, we studied five genes contributing to immunity, with polymorphism analyzed within protein coding regions (*Mhc-Drb*, *Tlr*s, *Mx2*) or in the promoter (*Tnf-*□). Variation at these immune-related genes has been shown to be associated with rodent responses to PUUV infections (35).

Our study first enabled to investigate the relative role of neutral processes and selection in shaping the geographic variation of immune gene variability in this cyclic bank vole metapopulation. As predicted under genetic drift only, reduction of immune-related gene variability was observed at *Mhc-Drb* gene during the crash year 2009, and it was of similar amplitude than

the decrease observed at microsatellites. We also noted a particular allele present at low frequencies in one site during the 2005 peak year could be lost and never recovered within the metapopulation after the 2006 crash. Such impact of genetic drift was also detected on SNPs, with different patterns detected according to the immune-related gene considered. Loss of less frequent variants was for example locally observed after the 2006 crash at *Mx2*_162 SNP only. However, this impact of genetic drift on immune-related genes seemed minor and very transient, as there were no such significant temporal changes in allelic frequencies at *Mhc-Drb* or other SNPs. This contrasts with the conclusion drawn from the meta-analysis of Sutton et al. (6). They proposed that the greater reduction in *Mhc* gene diversity compared to neutral genetic diversity may be observed when negative frequency-dependent selection acting before bottlenecks results in the uneven distribution of most *Mhc* variants/haplotype, accelerating the loss of *Mhc* variability.

Dispersal can be invoked to explain that allelic diversity was recovered once vole abundance increased, as previously seen in Winternitz et al. (9). The detection of previously unseen *Mhc-Drb* haplotypes in particular sites of the metapopulation during the 2008 peak year corroborated this possibility, assuming that it resulted from the immigration of bank voles from outside the metapopulation, carrying these different haplotypes.

Further model-based simulations revealed marginal departures from neutrality for several immune-related gene polymorphisms. They could reveal complex signatures of balancing or positive selection according to the genes and years / cycle phases considered. A marginal footprint of positive selection was detected at the -296 SNP of *Tnf-*□ promoter in 2007 only. *Tnf-*□ gene encodes for a cytokine named TNF-α, mediating both acute and chronic inflammatory responses, therefore promoting resistance against a number of infectious agents on one hand. On the other hand, over-production of TNF-α can have important pathological effects and has been associated in humans to the severity of malaria (100) and of hemorrhagic fevers with renal syndrome (101), although the opposite pattern has been observed in Belgian PUUV cases (102). Changes in the production of this cytokine should hence have important effects on individual fitness (103). We previously showed that polymorphism at the -296 SNP of *Tnf-*□ promoter was associated with changes in *Tnf-*□ expression levels and susceptibility to PUUV (63,104). As such, this SNP should

evolve under strong selection, potentially driven by pathogen-mediated pressure and/or energetic trade-offs between costly immunity (pro-inflammatory response) and other non-immune costly life history traits.

The *Tlr4*-1662 SNP showed signature of positive selection in 2008. *Tlr4* is part of *Tlrs* gene family and is involved in coevolutionary processes with a wide variety of pathogens (105,106). Several studies recently emphasized the impact of historical and contemporary positive selection on *Tlr4* gene polymorphism in rodents (94,107,108), and it is likely that pathogens might mediate this selection. The signature of positive selection observed in this study might reflect spatial heterogeneity in the whole pathogen community or in one/few pathogens recognized by TLR4. Nevertheless, because positive selection was observed in 2008, a peak year, when gene flow is important during spring when voles mature, and expected to homogenize directly transmitted pathogens, candidates should preferentially be searched among vector-borne agents (e.g. bacteria like *Bartonella* sp., *Borrelia* sp.) or pathogens able to survive outside their hosts (e.g. ectoparasites).

Finally, a marginally significant pattern of balancing selection was observed at *Mx2* gene in 2008 and we found a tendency for PUUV reassortants to be associated with a particular *Mx2* genotype. *Mx2* gene encodes for proteins that provide immunity against viruses replicating in the cytoplasm, including hantaviruses (109,110). The SNP detected under selection and associated with PUUV variants was located within the leucine zipper motif of the C-terminal GTP effector domain, where mutations can affect the antiviral efficacy of Mx proteins (111–113). Balancing selection could be mediated by spatiotemporal heterogeneity in candidate viruses, and it would be stronger during peak year when dispersal may homogenize their distribution within the area. We previously showed that the levels of *Mx2* gene expression were negatively correlated with PUUV prevalence in France (104). It would therefore be interesting to deepen our understanding of the influence of *Mx2* sequence and expression polymorphism on PUUV epidemiology, and in particular to investigate the mechanisms underlying the observed associations between *Mx2* polymorphism and PUUV reassortments (see (38,39).

Such a diversity of patterns has previously been described in arvicoline rodents experiencing population cycles. Bryja et al. (13) found density-dependent changes in selection pressure throughout a complete density cycle of the montane water vole (*Arvicola scherman*), and these changes were detected at only one *Mhc* class II gene over the two examined. In cyclic populations of field vole (*Microtus agrestis*), Turner et al. (94) detected signature of selection acting on only two genes encoding cytokines over the twelve immune-related genes examined. This variability in observed patterns could be mediated by different pathogens affecting different parts of the genome and temporal heterogeneity in pathogen pressure (e.g. (114) that may have a strong selective effect even in a few generations (e.g. (8). Nevertheless, we have to take these results cautiously as some of the underlying assumptions of our tests to detect departures from neutral expectation are likely to be violated in this study. In particular, FDIST2 and the modified DFDIST are based on an island model at migration-drift equilibrium, while the true demographic history of *M. glareolus* is characterized by non-equilibrium population dynamics. However, we have shown by means of simulations (see Supplementary Appendix S1 and Supplementary Fig. S3) that the approach was robust to temporal variations in population size, at least in the range of differentiation level observed in our data, which is consistent with the idea that the distribution of F_{ST} estimates should be robust to the vagaries of demographic history (115). At larger geographical scales, other characteristics of bank vole demographic history, including isolation by distance or range expansion, could lead to high false-positive rates for F_{ST} outlier methods that assume evolutionary-independent samples (116).

Conclusions

This study provided evidence for the role of vole dispersal on PUUV circulation through sex-specific and density-dependent movements. We also revealed that multiannual dynamic cycles were likely to affect selection acting on immune-related genes involved in susceptibility to PUUV. In the future, we recommend to develop such population genetics approaches based on neutral and immune-related genes in heterogeneous landscapes to better assess the influence of selection. We also advocate for high-throughput characterization of rodent microbial communities as it will

offer new opportunities to better understand the potential influence of pathogens as drivers of this selection, and in turn, rodent/hantavirus interactions.

Supporting Information

S1 Protocol: SNPs identification and genotyping

S1 Table: Characteristics and genetic diversity estimates within each year and each sampling site, including the number of bank voles sampled (N) and PUUV positives (Ni), PUUV seroprevalence and the genetic diversity estimates (H_o, H_e, F_{IS}, N_a). When less than eight individuals were sampled in a site, local estimates were not calculated (- and all the sites in 2009). 'Total' refers to the whole metapopulation. Significant values are in bold.

S2 Table: Analyses of single nucleotide polymorphism for four immune-related genes. A) Primers used for *M. glareolus* identification, amplification of gDNA for PCR and sequencing with corresponding fragment length and total length of the sequence. B) Polymorphism for three immune-related genes screened using a sample of 12 to 29 individuals from three European bank vole populations. Singletons (polymorphism was detected in only one heterozygote indivduals) were not included in further genotyping analyses of Konnevesi populations. The software PolyPhen (http://genetics.bwh.harvard.edu/ pph; Ramensky et al. 2002) was used to predict the functional impact of non-synonymous SNPs on the translated protein, based on biochemical and physical characteristics of the amino acid replacements.

S3 Table: Cycling conditions of PCRs.

S4 Table: Results of the two linear mixed models. Only significant pairwise interactions are reported.

S5 Table: F_{ST} estimates between sites per year (lower side) and associated *p*-values of Fisher exact tests (upper side).

S6 Table. F_{ST} estimates between years over the whole metapopulation (lower side) and associated *p*-values of Fisher exact tests (upper side).

S7 Table: This file includes A) the individual and spatial data of all bank voles, B) the microsatellite genotypes for 19 loci, C) the genotypic data for four immune-related genes (eight independent SNPs genotyped using the KASPar technology) and D) the *Mhc-Drb* exon 2 genotypes (sequences are available in Genbank).

S1 Figure: Distribution of F_{ST} conditional on the overall heterozygosity (H_e) at microsatellites, for the whole metapopulation dataset in 2005, 2007 and 2008. Black dots represent the observed, locus-specific, estimates of differentiation and heterozygosity for microsatellites. The 90%, 95% and 99% confidence regions of the null distribution (obtained by means of stochastic simulations in a neutral model) are shown in dark grey, medium grey and light grey, respectively. The density was obtained using the Average Shifted Histogram (ASH) algorithm (79) with smoothing parameter m = 2.

S2 Figure: Phylogenetic relationships of bank vole 454 (202 bp)-DRB sequences (this study; Mygl-DRB*120–151) and previously known Cluster I, Cluster II and Group III bank vole sequences from (62); Clgl-DRB*01-28 (eliding the numbers 2 and 9); EF434791–EF434816] expressed as neighbour-joining tree based on Kimura's two-parameter distances, pairwise deletion. Bootstrap values are based on 1,000 replicates. Species specific Mhc nomenclature is used. H2 IEb (Mus musculus DRB: U28489.1) serves as outgroup.

S3 Figure: Distribution of F_{ST} conditional on the overall heterozygosity (H_e) at immune-related genes, for the whole metapopulation dataset in 2007 and 2008, for different demographic scenarios: constant deme size (A-B), cyclic deme size (C-D) and randomly-varying deme size (E-F). See Supplementary Appendix S1 for further details on the simulations. Black dots represent the observed, locus-specific, estimates of differentiation and heterozygosity for SNPs in candidate genes. The 90%, 95% and 99% confidence regions of the null distribution (obtained by means of stochastic simulations in a neutral model) are shown in dark grey, medium grey and light grey, respectively. The density was obtained using the average shifted histogram (ASH) algorithm (79) with smoothing parameter m = 2.

S1 Appendix: This file includes details on the simulations performed to investigate to what extent the modified DFDIST approach to detect signatures of selection was robust to temporal variations in population size.

Acknowledgments

Microsatellite data used in this work were produced through the technical facilities of the Centre Méditerranéen Environnement Biodiversité (CeMEB). We are grateful to Audrey Rohfritsch and Viola Walther for the identification of SNPs at immune gene during the pilot study. We are grateful to Jeremy Gaudin for technical assistance and preliminary analyses.

Fundings

This research has been partially funded by EU grants GOCE-CT-2003- 010284 EDEN and FP7-261504 EDENext, and the paper is catalogued by the EDENext Steering Committee as EDENext 405 (http://www.edenext.eu). AD is currently funded by an INRA-EFPA / ANSES fellowship.

Author Contributions

Conceived and designed the vole sampling survey, analyzed PUUV serology: HH, JN, MR, LV. Conceived and designed the molecular analyses: AD, MG, JFC, EG, NC. Analyzed the data: AD, BG, RV, EG. Wrote the paper: AD, NC, BG, RV. LV, HH, MR and JFC helped to improve and draft the manuscript. All authors have read and approved the final manuscript.

References

1. Archie E a, Luikart G, Ezenwa VO. Infecting epidemiology with genetics: a new frontier in disease ecology. Trends Ecol Evol. 2009;24(1):21–30.

2. Price PW. Evolutionary biology of parasites (Vol. 15). Princeton University Press; 1980. 237 p.

3. Biek R, Real L. The landscape genetics of infectious disease emergence and spread. Mol Ecol. 2010;19(17):3515–31.

4. Charbonnel N, Cosson J-F. Molecular Epidemiology of Disease Resistance Genes with Perspectives for Researches on Biological Invasions and Hybrid Zones. In: S M, Beaudeau F, Cabaret J, de Rycke J, editors. New Frontiers of Molecular Epidemiology of Infectious Diseases. Dordrecht: Springer Netherlands; 2011. p. 255–90.

5. Ejsmond MJ, Radwan J. MHC diversity in bottlenecked populations: a simulation model.

Conserv Genet. 2011;12(1):129–37.

6. Sutton JT, Nakagawa S, Robertson BC, Jamieson IG. Disentangling the roles of natural selection and genetic drift in shaping variation at MHC immunity genes. Mol Ecol. 2011;20(21):4408–20.

7. Grueber CE, Wallis GP, Jamieson IG. Genetic drift outweighs natural selection at toll-like receptor (TLR) immunity loci in a re-introduced population of a threatened species. Mol Ecol. 2013;22(17):4470–82.

8. Oliver MK, Piertney SB. Selection maintains MHC diversity through a natural population bottleneck. Mol Biol Evol. 2012;29(7):1713–20.

9. Winternitz JC, Wares JP, Yabsley MJ, Altizer S. Wild cyclic voles maintain high neutral and MHC diversity without strong evidence for parasite-mediated selection. Evol Ecol. 2014;28:957–75.

10. Frankham R. Effective population size/adult population size ratios in wildlife: a review. Genet Res. 1995;66(2):95–107.

11. Nei M, Maruyama T, Chakraborty R. The bottleneck effect and genetic variability in populations. Evolution (N Y). 1975;29:1–10.

12. Maruyama T, Fuerst PA. Population bottlenecks and nonequilibrium models in population genetics. II. Number of alleles in a small population that was formed by a recent bottleneck. Genetics. 1985;111:675–89.

13. Bryja J, Charbonnel N, Berthier K, Galan M, Cosson JF. Density-related changes in selection pattern for major histocompatibility complex genes in fluctuating populations of voles. Mol Ecol. 2007;16:5084–97.

14. Burton C, Krebs CJ, Taylor EB. Population genetic structure of the cyclic snowshoe hare (Lepus americanus) in southwestern Yukon, Canada. Mol Ecol. 2002;11:1689–701.

15. Berthier K, Charbonnel N, Galan M, Chaval Y, Cosson J-F. Migration and recovery of the genetic diversity during the increasing density phase in cyclic vole populations. Mol Ecol. 2006;15:2665–76.

16. Ehrich D, Yoccoz NG, Ims RA. Multi-annual density fluctuations and habitat size enhance genetic variability in two northern voles. Oikos. 2009;118(10):1441–52.

17. Rikalainen K, Aspi J, Galarza J a, Koskela E, Mappes T. Maintenance of genetic diversity in cyclic populations-a longitudinal analysis in Myodes glareolus. Ecol Evol. 2012;2(7):1491–

502.

18. Gauffre B, Berthier K, Inchausti P, Chaval Y, Bretagnolle V, Cosson JF. Short-term variations in gene flow related to cyclic density fluctuations in the common vole. Mol Ecol. 2014;23:3214–25.

19. Berthier K, Galan M, Foltête JC, Charbonnel N, Cosson JF. Genetic structure of the cyclic fossorial water vole (Arvicola terrestris): landscape and demographic influences. Mol Ecol. 2005;14(9):2861–71.

20. Hanski I, Henttonen H. Population cycles of small rodents in Fennoscandia. In: Berryman A, editor. Populations cycles: the case for trophic interactions. 2002. p. 44–68.

21. Henttonen H, McGuire AD, Hansson L. Spectral analyses on density variations. Vol. 22, Ann. Zool. Fennici. 1985. p. 221–7.

22. Vaheri A, Henttonen H, Voutilainen L, Mustonen J, Sironen T, Vapalahti O. Hantavirus infections in Europe and their impact on public health. Rev Med Virol Virol. 2012;23(1):35–49.

23. Bernshtein AD, Apekina NS, Mikhailova T V., Myasnikov YA, Khlyap LA, Korotkov YS, et al. Dynamics of Puumala hantavirus infection in naturally infected bank voles (Clethrinomys glareolus). Arch Virol. 1999;144(12):2415–28.

24. Kallio ER, Klingström J, Gustafsson E, Manni T, Vaheri A, Henttonen H, et al. Prolonged survival of Puumala hantavirus outside the host: Evidence for indirect transmission via the environment. J Gen Virol. 2006;87(8):2127–34.

25. Voutilainen L, Sironen T, Tonteri E, Tuiskunen Back A, Razzauti M, Karlsson M, et al. Life-Long Shedding of Puumala Hantavirus in Wild Bank Voles (Myodes glareolus). J Gen Virol. 2015;96(6):1438–47.

26. Bernshtein AD, Apekina NS, Mikhailova T V., Myasnikov YA, Khlyap LA, Korotkov YS, et al. Dynamics of Puumala hantavirus infection in naturally infected bank voles (Clethrinomys glareolus). Arch Virol. 1999;144(12):2415–28.

27. Meyer BJ, Schmaljohn CS. Persistent hantavirus infections: characteristics and mechanisms. Trends Microbiol. 2000;8(2):61–7.

28. Kallio ER, Voutilainen L, Vapalahti O, Vaheri A, Henttonen H, Koskela E, et al. Endemic hantavirus infection impairs the winter survival of its rodent host. Ecology. 2007;88(8):1911–6.

29. Kallio ER, Helle H, Koskela E, Mappes T, Vapalahti O. Age-related effects of chronic hantavirus infection on female host fecundity. J Anim Ecol. 2015;84(5):1264–72.

30. Tersago K, Crespin L, Verhagen R, Leirs H. Impact of Puumala virus infection on maturation and survival in bank voles: a capture-mark-recapture analysis. J Wildl Dis. 2012;48(1):148–56.

31. Voutilainen L, Kallio ER, Niemimaa J, Vapalahti O, Henttonen H. Temporal dynamics of Puumala hantavirus infection in cyclic populations of bank voles. Sci Rep. 2016;6.

32. Guivier E, Galan M, Chaval Y, Xuéreb A, Ribas Salvador A, Poulle M-L, et al. Landscape genetics highlights the role of bank vole metapopulation dynamics in the epidemiology of Puumala hantavirus. Mol Ecol. 2011;20(17):3569–83.

33. Clement J, Maes P, Van Ypersele De Strihou C, Van Der Groen G, Barrios JM, Verstraeten WW, et al. Beechnuts and outbreaks of nephropathia epidemica (NE): Of mast, mice and men. Nephrol Dial Transplant. 2010;25(6):1740–6.

34. Weber de Melo V, Sheikh Ali H, Freise J, Kühnert D, Essbauer S, Mertens M, et al. Spatiotemporal dynamics of Puumala hantavirus associated with its rodent host, Myodes glareolus. Evol Appl. 2015;8(6):545–59.

35. Charbonnel N, Pagès M, Sironen T, Henttonen H, Vapalahti O, Mustonen J, et al. Immunogenetic factors affecting susceptibility of humans and rodents to hantaviruses and the clinical course of hantaviral disease in humans. Viruses. 2014;6(5):2214–41.

36. Deter J, Chaval Y, Galan M, Gauffre B, Morand S, Henttonen H, et al. Kinship, dispersal and hantavirus transmission in bank and common voles. Arch Virol. 2008;153(3):435–44.

37. Voutilainen L, Sironen T, Tonteri E, Bäck AT, Razzauti M, Karlsson M, et al. Life-long shedding of Puumala hantavirus in wild bank voles (Myodes glareolus). J Gen Virol. 2015;96(2015):1238–47.

38. Razzauti M, Plyusnina A, Henttonen H, Plyusnin A. Accumulation of point mutations and reassortment of genomic RNA segments are involved in the microevolution of Puumala hantavirus in a bank vole (Myodes glareolus) population. J Gen Virol . 2008;89:1649–60.

39. Razzauti M, Plyusnina A, Henttonen H, Plyusnin A. Microevolution of Puumala hantavirus during a complete population cycle of its host, the bank vole (Myodes glareolus). PLoS One. 2013;8(5):e64447.

40. Kallio-Kokko H, Laakkonen J, Rizzoli a, Tagliapietra V, Cattadori I, Perkins SE, et al. Hantavirus and arenavirus antibody prevalence in rodents and humans in Trentino, Northern

Italy. Epidemiol Infect. 2006;134(4):830–6.

41. Kallio ER, Poikonen A, Vaheri A, Vapalahti O, Henttonen H, Koskela E, et al. Maternal antibodies postpone hantavirus infection and enhance individual breeding success. Proc R Soc B Biol Sci. 2006;273:2771–6.

42. Rikalainen K, Grapputo a, Knott E, Koskela E, Mappes T. A large panel of novel microsatellite markers for the bank vole (Myodes glareolus). Mol Ecol Resour. 2008;8(5):1164–8.

43. Rohfritsch A, Guivier E, Galan M, Chaval Y, Cosson J-F, Charbonnel N. Apport de l'immunogénétique à la compréhension des interations entre le campagnol roussâtre Myodes glareolus et l'hantavirus Puumala. Bull Acad Vet Fr. Académie vétérinaire de France; 2013;166(2):171–83.

44. Klein J, O'Huigin C. MHC polymorphism and parasites. Philos Trans R Soc Lond B Biol Sci. 1994;346(1317):351–7.

45. Ayres JS, Schneider DS. Tolerance of infections. Annu Rev Immunol. 2012;30:271–94.

46. Wlasiuk G, Nachman MW. Adaptation and constraint at toll-like receptors in primates. Mol Biol Evol. 2010;27(9):2172–86.

47. Sabeti PC, Varilly P, Fry B, Lohmueller J, Hostetter E, Cotsapas C, et al. Genome-wide detection and characterization of positive selection in human populations. Nature. 2007;449(7164):913–8.

48. Bowie AG, Haga IR. The role of Toll-like receptors in the host response to viruses. Mol Immunol. 2005;42(8):859–67.

49. Vassalli P. The pathophysiology of Tumor Necrosis Factor. Annu Rev Immunol. 1992;10:411–52.

50. Bouma G, Crusius JB, Oudkerk Pool M, Kolkman JJ, von Blomberg BM, Kostense PJ, et al. Secretion of tumour necrosis factor alpha and lymphotoxin alpha in relation to polymorphisms in the TNF genes and HLA-DR alleles. Relevance for inflammatory bowel disease. Scand J Immunol. 1996;43(4):456–63.

51. Wilson a G, Symons J a, McDowell TL, McDevitt HO, Duff GW. Effects of a polymorphism in the human tumor necrosis factor alpha promoter on transcriptional activation. Proc Natl Acad Sci U S A. 1997;94(7):3195–9.

52. Jin HK, Takada a, Kon Y, Haller O, Watanabe T. Identification of the murine Mx2 gene:

interferon-induced expression of the Mx2 protein from the feral mouse gene confers resistance to vesicular stomatitis virus. J Virol. 1999;73(6):4925–30.

53. Porter BF, Ambrus a, Storts RW. Immunohistochemical evaluation of mx protein expression in canine encephalitides. Vet Pathol. 2006;43(6):981–7.

54. Galan M, Guivier E, Caraux G, Charbonnel N, Cosson J-F. A 454 multiplex sequencing method for rapid and reliable genotyping of highly polymorphic genes in large-scale studies. BMC Genomics. 2010;11.

55. Schad J, Sommer S, Ganzhorn JU. MHC Variability of a Small Lemur in the Littoral Forest Fragments of Southeastern Madagascar. Conserv Genet. 2004;5(3):299–309.

56. Galan M, Pagès M, Cosson J-F. Next-generation sequencing for rodent barcoding: species identification from fresh, degraded and environmental samples. PLoS One. 2012;7(11).

57. Piry S, Guivier E, Realini a, Martin J-F. |SE|S|AM|E| Barcode: NGS-oriented software for amplicon characterization--application to species and environmental barcoding. Mol Ecol Resour. 2012;12(6):1151–7.

58. Hall TA. BioEdit: a user-friendly biological sequence alignment editor and analysis program for Windows 95/98/NT. Nucleic Acids Symp Ser. 1999;41:95–8.

59. Chenna R, Sugawara H, Koike T, Lopez R, Gibson TJ, Higgins DG, et al. Multiple sequence alignment with the Clustal series of programs. Nucleic Acids Res. 2003;31(13):3497–500.

60. Klein J, Bontrop RE, Dawkins RL, Erlich HA, Gyllensten UB, Heise ER, et al. Nomenclature for the major histocompatibility complexes of different species: a proposal. In: The HLA System in Clinical Transplantation. Springer Berlin Heidelberg.; 1993. p. 407–11.

61. Tamura K, Dudley J, Nei M, Kumar S. MEGA4: Molecular Evolutionary Genetics Analysis (MEGA) software version 4.0. Mol Biol Evol. 2007;24(8):1596–9.

62. Axtner J, Sommer S. Gene duplication, allelic diversity, selection processes and adaptive value of MHC class II DRB genes of the bank vole, Clethrionomys glareolus. Immunogenetics. 2007;59(5):417–26.

63. Guivier E, Galan M, Salvador AR, Xuéreb A, Chaval Y, Olsson GE, et al. Tnf-α expression and promoter sequences reflect the balance of tolerance/resistance to Puumala hantavirus infection in European bank vole populations. Infect Genet Evol. 2010;10(8):1208–17.

64. Kloch A, Babik W, Bajer A, Siński E, Radwan J. Effects of an MHC-DRB genotype and allele number on the load of gut parasites in the bank vole Myodes glareolus. Mol Ecol.

2010;19(Suppl 1):255–65.

65. Scherman K, Raberg L, Westerdahl H. Positive selection on MHC class II DRB and DQB genes in the bank vole (Myodes glareolus). J Mol Evol. 2014;78(5):293–305.

66. Bollmer JL, Ruder EA, Johnson JA, Eimes JA, Dunn PO. Drift and selection influence geographic variation at immune loci of prairie-chickens. Mol Ecol. 2011;4695–706.

67. Quéméré E, Galan M, Cosson J-F, Klein F, Aulagnier S, Gilot-Fromont E, et al. Immunogenetic heterogeneity in a widespread ungulate: the European roe deer (*Capreolus capreolus*). Mol Ecol. 2015;24(15):3873–87.

68. Ramensky V, Bork P, Sunyaev S. Human non-synonymous SNPs: server and survey. Nucleic Acids Res. 2002;30(17):3894–900.

69. Raymond M, Rousset F. An exact test for population differentiation. Evolution (N Y). 1995;49(6):1283–1283.

70. Benjamini Y, Hochberg Y. Controlling the False Discovery Rate : A Practical and Powerful Approach to Multiple Testing. J R Stat Soc. 1995;57(1):289–300.

71. Goudet J. FSTAT (version 1.2): a computer program to cal culate F-statistics. J Hered. 1995;86:485–6.

72. El Mousadik A, Petit R. High level of genetic differentiation for allelic richness among populations of the argan tree [Argania spinosa (L.) Skeels] endemic to Morocco. Theor Appl Genet. 1996;92:832–9.

73. Nei M. Estimation of average heterozygosity and genetic distance from a small number of individuals. Genetics. 1978;89(3):583–90.

74. Weir B., Cockerham C. Estimating F-statistics for the analysis of population structure. Evolution (N Y). 1984;38(6):1358–70.

75. Belkhir K, Borsa P, Chikhi L, Raufaste N, Bonhomme F. GENETIX 4.05, logiciel sous Windows TM pour la génétique des populations. 1996. Laboratoire génome, populations, interactions, CNRS UMR.

76. R Core Team. R: A language and environment for statistical computing. 2013.

77. Beaumont M a., Nichols R a. Evaluating Loci for Use in the Genetic Analysis of Population Structure. Proc R Soc B Biol Sci. 1996;263(1377):1619–26.

78. Ségurel L, Lafosse S, Heyer E, Vitalis R. Frequency of the AGT Pro11Leu polymorphism in

humans: Does diet matter? Ann Hum Genet. 2010;74(1):57–64.

79. Scott D. Multivariate Density Estimation: Theory, Practice, and Visualization. New York: 2002. 317 p.

80. Foll M, Gaggiotti O. Identifying the Environmental Factors That Determine the Genetic Structure of Populations. Genetics. 2006;174(2):875–91.

81. Excoffier L, Lischer HEL. Arlequin suite ver 3.5: a new series of programs to perform population genetics analyses under Linux and Windows. Mol Ecol Resour. 2010;10(3):564–7.

82. Pritchard JK, Stephens M, Donnelly P. Inference of population structure using multilocus genotype data. Genetics. 2000;155(2):945–59.

83. Evanno G, Regnaut S, Goudet J. Detecting the number of clusters of individuals using the software STRUCTURE: a simulation study. Mol Ecol. 2005;14(8):2611–20.

84. Jakobsson M, Rosenberg N a. CLUMPP: a cluster matching and permutation program for dealing with label switching and multimodality in analysis of population structure. Bioinformatics. 2007;23(14):1801–6.

85. Rosenberg NA. Distruct : a program for the graphical display of population structure. Mol Ecol Notes. 2004;4(1):137-8

86. Li CC, Weeks DE, Chakravarti A. Similarity of DNA finger prints due to chance and relatedness. Hum Hered. 1993;43:45–52.

87. Hardy O, Vekemans X. SPAGeDi: a versatile computer program to analyse spatial genetic structure at the individual or population levels. Mol Ecol Notes. 2002;2:618–20.

88. Vekemans X, Hardy OJ. New insights from fine-scale spatial genetic structure analyses in plant populations. Mol Ecol. 2004;13(4):921–35.

89. Prugnolle F, Meeûs T De. Inferring sex-biased dispersal from population genetic tools: a review. Heredity (Edinb). 2002;161–5.

90. Coulon A, Cosson J-F, Morellet N, Angibault J-M, Cargnelutti B, Galan M, et al. Dispersal is not female biased in a resource-defence mating ungulate, the European roe deer. Proc Biol Sci . 2006;273(1584):341–8.

91. Hansson L. Geographic differences in the sociability of voles in relation to cyclicity. Anim Behav. 1986;34(4):1215–21.

92. Thioulouse J, Chessel D, Dolédec S, Olivier J. ADE-4: a multivariate analysis and graphical display software. Stat Comput. 1997;7:75–83.

93. Haldane BJ. The estimation and significance of the logarithm of a ratio of frequencies. Ann Hum Genet. 1956;20(4):309–11.

94. Turner AK, Begon M, Jackson J a., Paterson S. Evidence for selection at cytokine loci in a natural population of field voles (*Microtus agrestis*). Mol Ecol. 2012;21(7):1632–46.

95. Hansson B, Henttonen H. Rodent dynamics as community processes. Trends Ecol Evol. 1988;8:195–200.

96. Ehrich D, Jorde PE, Krebs CJ, Kenney a J, Stacy JE, Stenseth NC. Spatial structure of lemming populations (Dicrostonyx groenlandicus) fluctuating in density. Mol Ecol. 2001;10(2):481–95.

97. García-Navas V, Bonnet T, Waldvogel D, Wandeler P, Camenisch G, Postma E. Gene flow counteracts the effect of drift in a Swiss population of snow voles fluctuating in size. Biol Conserv.; 2015;191:168–77.

98. Pilot M, Dąbrowski MJ, Jancewicz E, Schtickzelle N, Gliwicz J. Temporally stable genetic variability and dynamic kinship structure in a fluctuating population of the root vole Microtus oeconomus. Mol Ecol. 2010;19:2800–12.

99. Le Galliard J, Rémy A, Ims R, Lambin X. Patterns and processes of dispersal behaviour in arvicoline rodents. Mol Ecol. 2012;21:505–23.

100. Kwiatkowski D, Hill a V, Sambou I, Twumasi P, Castracane J, Manogue KR, et al. TNF concentration in fatal cerebral, non-fatal cerebral, and uncomplicated Plasmodium falciparum malaria. Lancet. 1990;336(8725):1201–4.

101. Klingstrom J, Plyusnin A, Vaheri A, Lundkvist A. Wild-type Puumala hantavirus infection induces cytokines, C-reactive protein, creatinine, and nitric oxide in cynomolgus macaques. J Virol. 2002;76(1):444–9.

102. Maes P, Clement J, Groeneveld PHP, Colson P, Huizinga TWJ, Van Ranst M. Tumor necrosis factor-α genetic predisposing factors can influence clinical severity in nephropathia epidemica. Viral Immunol. 2006;19(3):558–64.

103. Knight JC, Kwiatkowski D. Inherited variability of tumor necrosis factor production and susceptibility to infectious disease. Proc Assoc Am Physicians. 1999;111(4):290–8.

104. Guivier E, Galan M, Henttonen H, Cosson J-F, Charbonnel N. Landscape features and

helminth co-infection shape bank vole immunoheterogeneity, with consequences for Puumala virus epidemiology. Heredity (Edinb); 2014;112(3):274–81.

105. Akira S, Uematsu S, Takeuchi O. Pathogen recognition and innate immunity. Cell. 2006;124(4):783–801.

106. Hughes AL, Piontkivska H. Functional diversification of the toll-like receptor gene family. Immunogenetics. 2008;60(5):249–56.

107. Fornůsková A, Bryja J, Vinkler M, Macholán M, Piálek J. Contrasting patterns of polymorphism and selection in bacterial-sensing toll-like receptor 4 in two house mouse subspecies. Ecol Evol. 2014;4(14):2931–44.

108. Fornůsková A, Vinkler M, Pagès M, Galan M, Jousselin E, Cerqueira F, et al. Contrasted evolutionary histories of two Toll-like receptors (Tlr4 and Tlr7) in wild rodents (MURINAE). BMC Evol Biol. 2013;13:194.

109. Jin HK, Yoshimatsu K, Takada A, Ogino M, Asano A, Arikawa J, et al. Mouse Mx2 protein inhibits hantavirus but not influenza virus replication. Arch Virol. 2001;146(1):41–9.

110. Lee SH, Vidal SM. Functional diversity of Mx proteins: Variations on a theme of host resistance to infection. Genome Res. 2002;12(4):527–30.

111. Janzen C, Kochs G, Haller O. A monomeric GTPase-negative MxA mutant with antiviral activity. J Virol. 2000;74(17):8202–6.

112. Kochs G, Haller O. Interferon-induced human MxA GTPase blocks nuclear import of Thogoto virus nucleocapsids. Proc Natl Acad Sci U S A. 1999;96(5):2082–6.

113. Zürcher T, Pavlovic J, Staeheli P. Mechanism of human MxA protein action: variants with changed antiviral properties. EMBO J. 1992;11(4):1657–61.

114. Fraser B, Ramnarine I, Neff B. Temporal variation at the Mhc class IIB in wild populations of the guppy (Poecilia reticulata). Evolution (N Y). 2010;64:2086–96.

115. Beaumont MA. Adaptation and speciation: What can Fst tell us? Trends Ecol Evol. 2005;20(8):435–40.

116. Lotterhos KE, Whitlock MC. Evaluation of demographic history and neutral parameterization on the performance of FST outlier tests. Mol Ecol. 2014;23(9):2178–92.

A

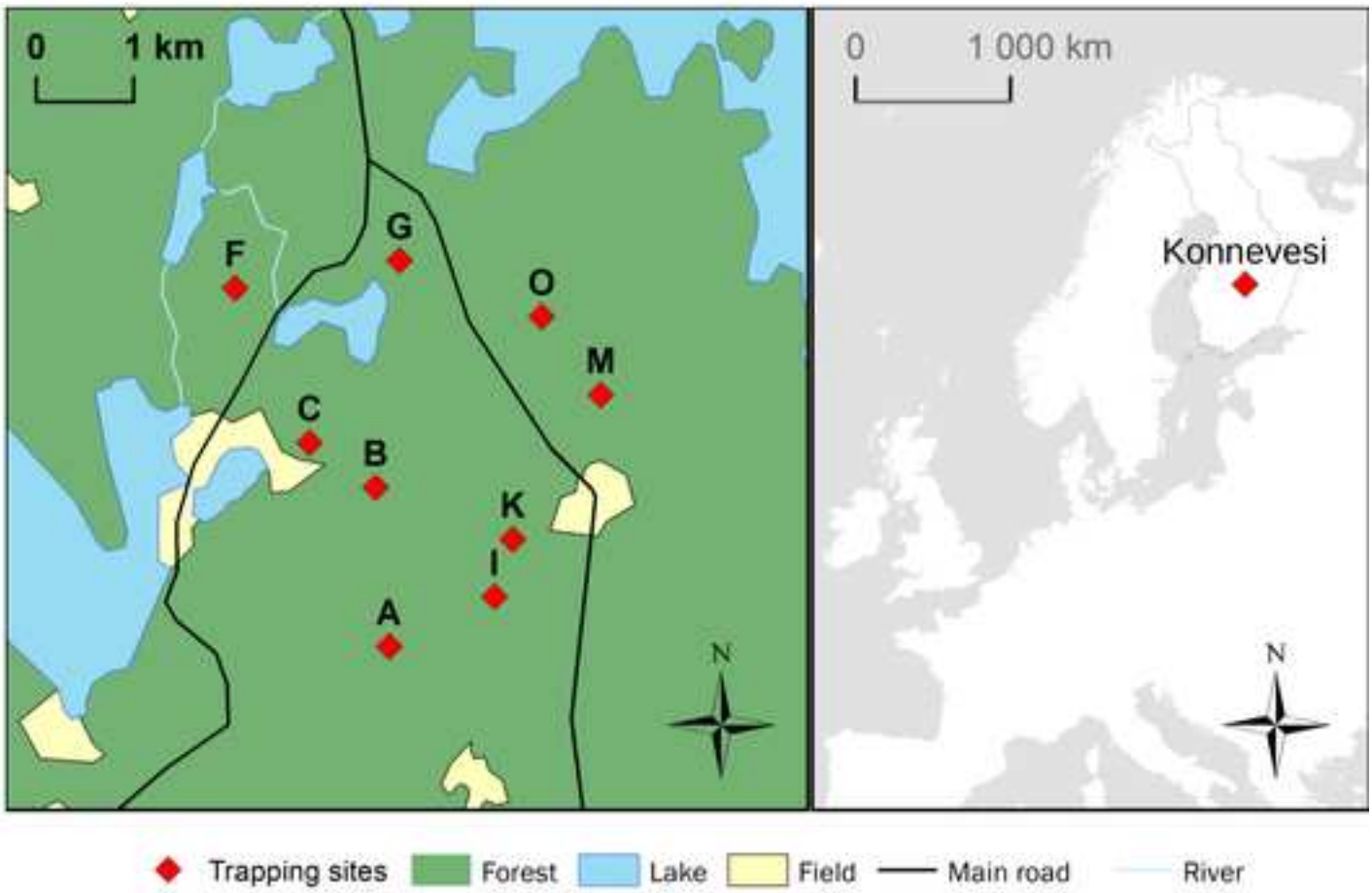
0 1 km
F
G
O
M
C
B
K
I
A
N
0 1 000 km
Konnevesi
N
Trapping sites
Forest
Lake
Field
Main road
River

B

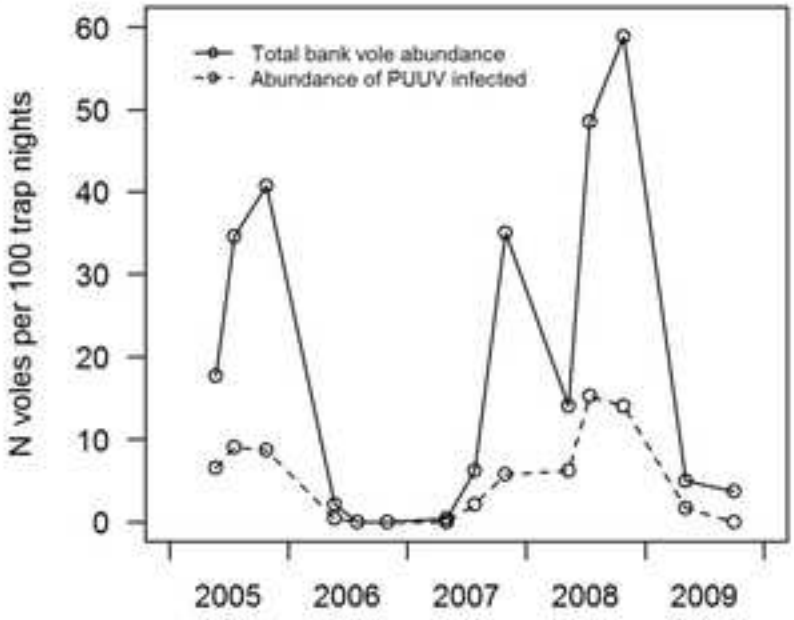
Total bank vole abundance
Abundance of PUUV infected
N voles per 100 trap nights
0
10
20
30
40
50
60
2005
2006
2007
2008
2009

Figure2

Click here to download Figure Figure2_Dubois.tiff

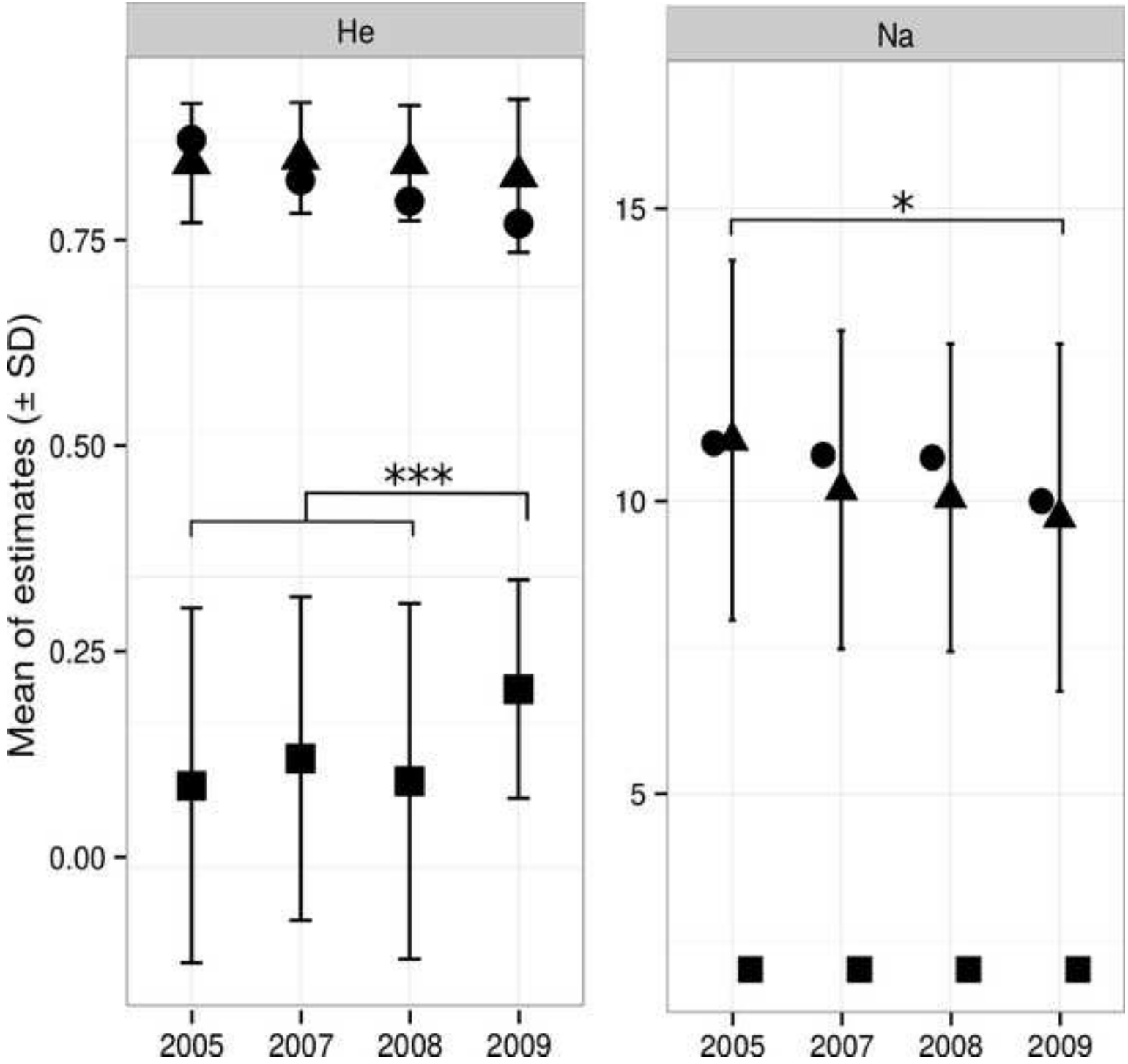

Figure3

Click here to download Figure Figure3_Dubois.tiff

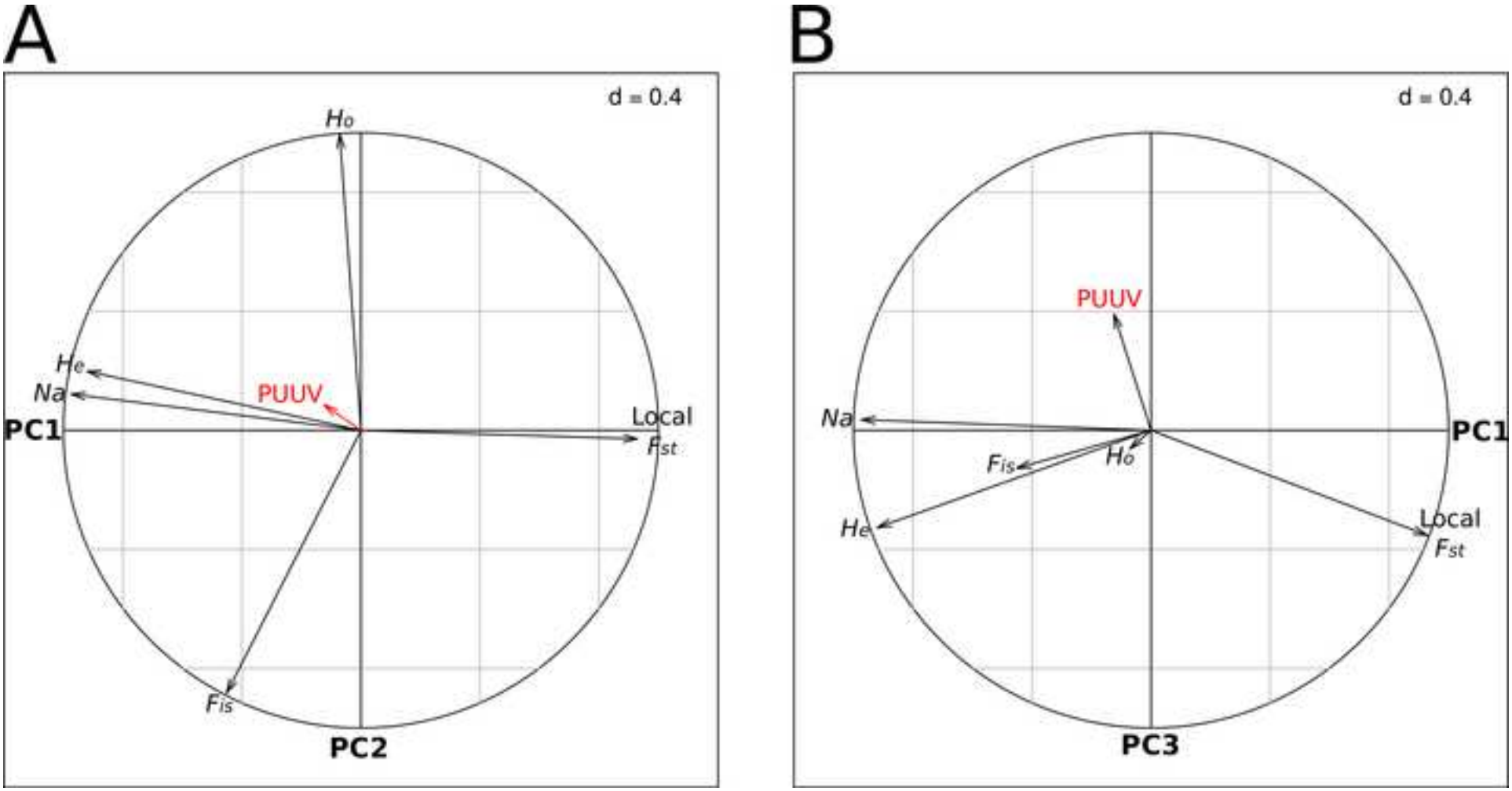

Figure4

Click here to download Figure Figure4_Dubois.tiff

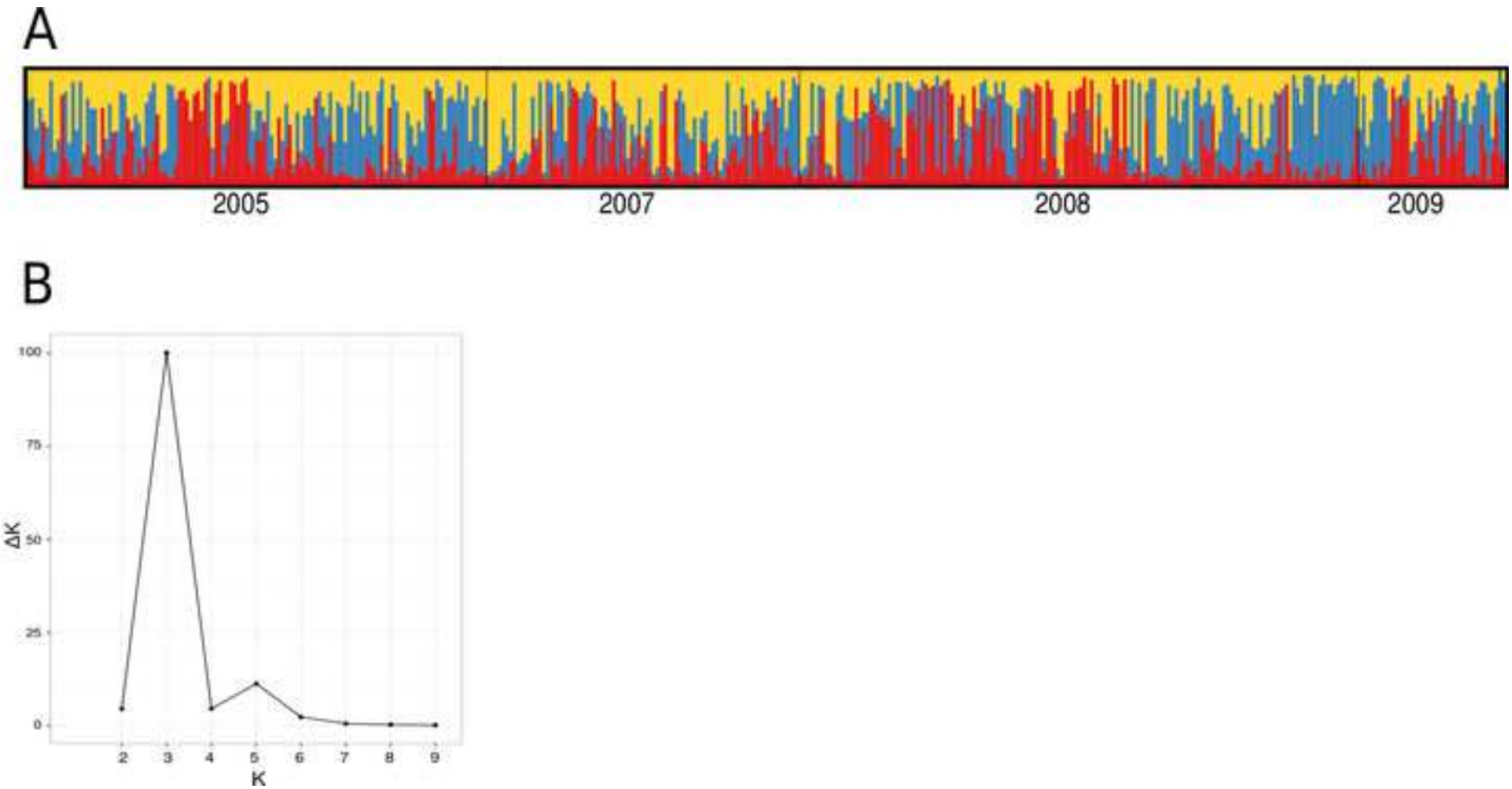

Figure5

Click here to download Figure Figure5_Dubois.tiff

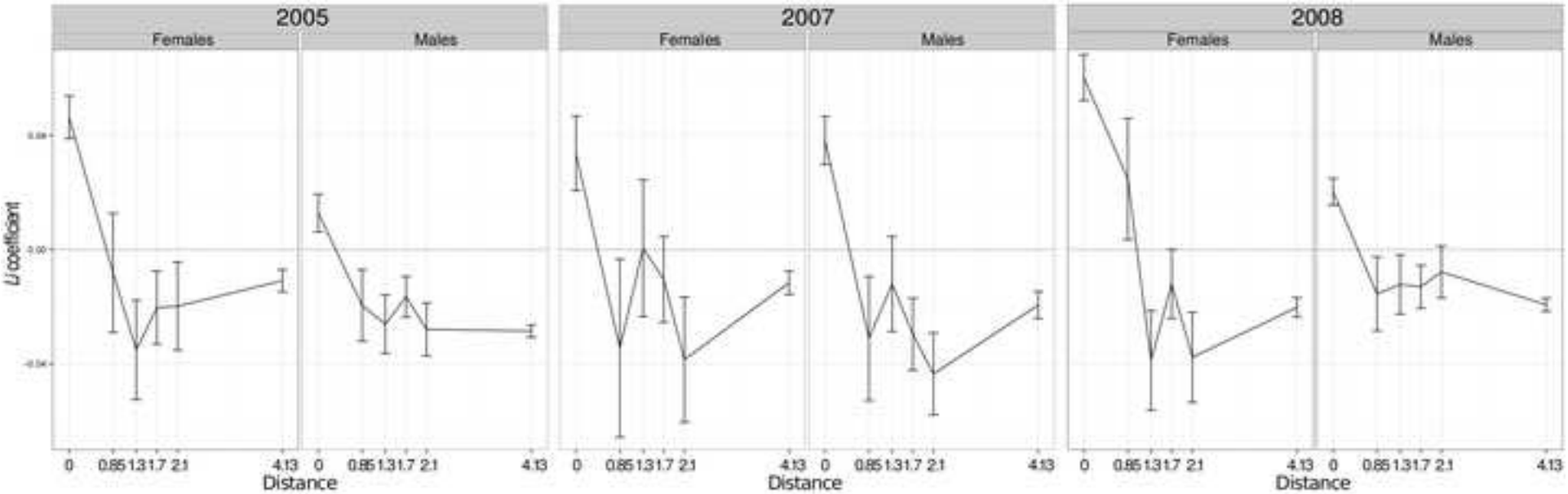

Figure6

Click here to download Figure Figure6_Dubois_Revised.pdf

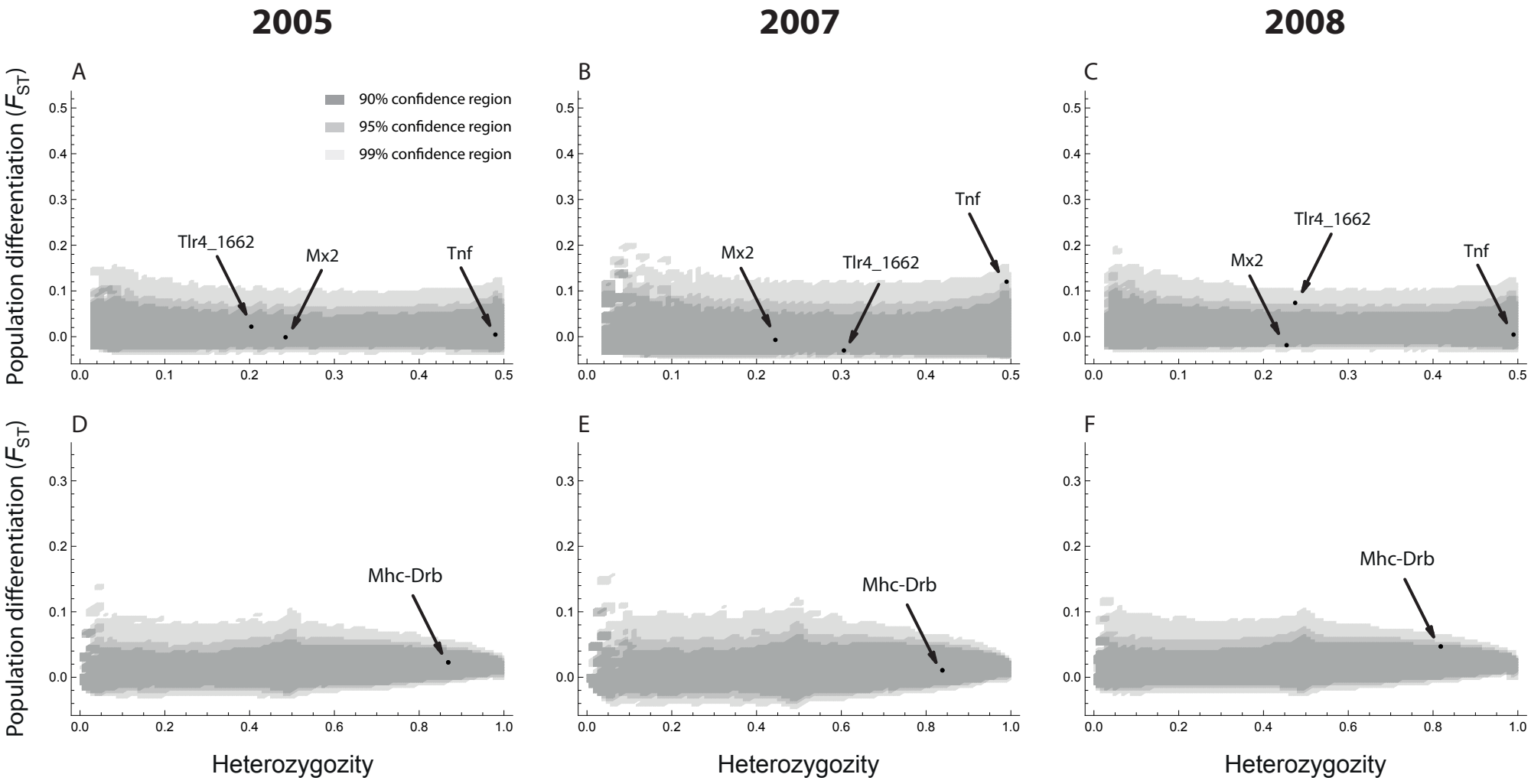

Figure7

Click here to download Figure Figure7_Dubois_Revised.tiff

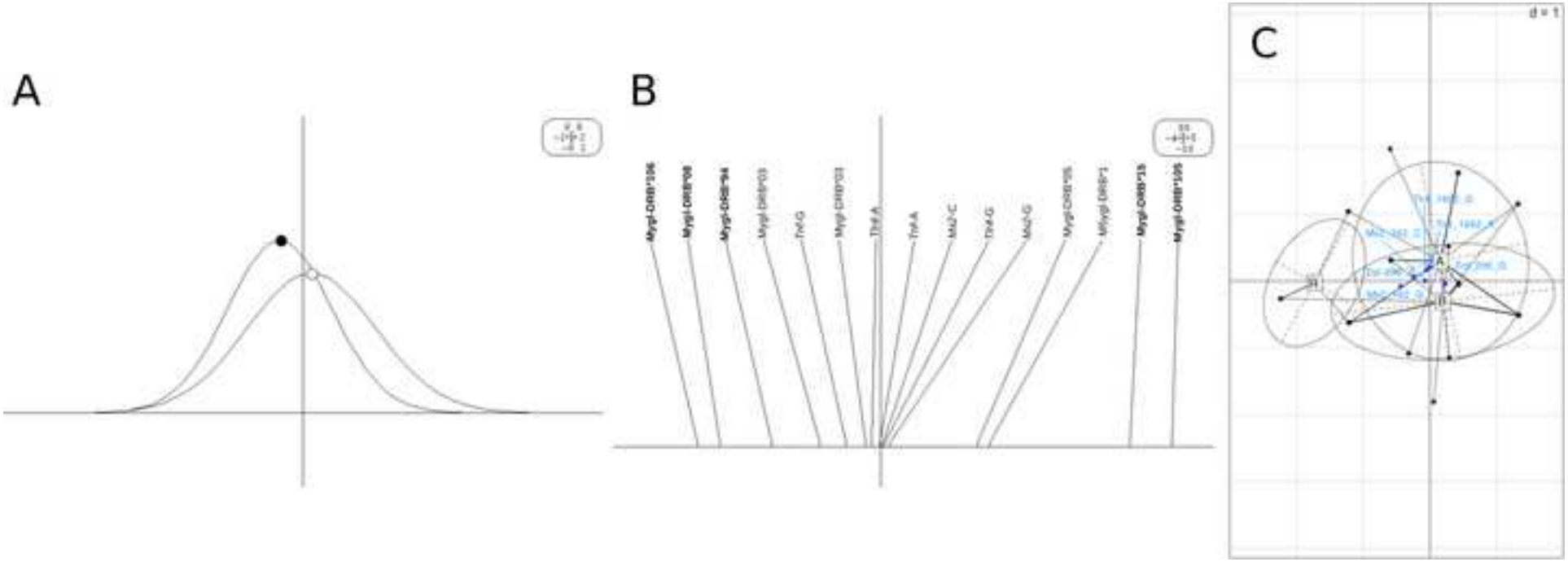

Click here to access/download
Supporting Information - Compressed/ZIP File Archive
Supplementary_data.zip